



UK Centre for
Ecology & Hydrology



VLAAMSE
MILIEUMAATSCHAPPIJ

Dry deposition measurements of ammonia at two heathland sites in Flanders (Nov 2021 – Dec 2024)

Final report

Chiara Di Marco, Jeroen Staelens, Marsailidh Twigg,
Amy Stephens, Eiko Nemitz

Issue Number 1

Date 20/05/2025

Client VMM

UKCEH reference VMMReport4/ 4

UKCEH contact details Chiara Di Marco
Bush Estate, Midlothian, EH26 0QB, UK

t: +44 131 4458588
e: cdma@ceh.ac.uk

Author Chiara Di Marco

Date 20/05/2025

This study was carried out on behalf of and in cooperation with Flanders Environment Agency (*Vlaamse Milieumaatschappij*, VMM). It contains the opinion of the authors and not necessarily that of Flanders Environment Agency.

Contents

List of symbols and abbreviations.....	2
1 Introduction.....	3
2 COTAG system	5
2.1 Principle of operation.....	5
2.2 The aerodynamic flux gradient method	6
2.3 Denuders.....	7
2.4 Analytical methodology	9
2.4.1 Preparation of samples and analysis	9
2.5 Quality control of NH ₃ concentrations: removal of outliers	9
2.6 Limitations	10
2.6.1 Delay in determining the stability class	10
2.6.2 Long-term sampling ignoring the “cross-term”.....	10
2.6.3 Conditional sampling ignoring fluxes in off-mode.....	11
2.6.4 Zero-plane displacement height.....	11
3 Sites description	13
3.1 Criteria for site selection.....	13
3.2 Maasmechelen (Mechelse Heide).....	13
3.3 Kalmthout (Kalmthoutse Heide)	15
3.4 COTAG system set up at VMM sites.....	16
4 Results	20
4.1 Wind roses	20
4.2 Data capture.....	21
4.3 NH ₃ concentrations	25
4.4 NH ₃ fluxes	30
4.5 Gap-filled NH ₃ deposition	32
4.6 Wind profile study.....	35
4.6.1 Methodology.....	35
4.6.2 Maasmechelen.....	36
4.6.3 Kalmthout.....	38
5 Conclusions & recommendations	42
Bibliography.....	43

List of symbols and abbreviations

a_{cross}	Cross-term correction coefficient
<i>A-Profile</i>	$(z-d)/L$ is within the stable/near-neutral window set for the site
<i>B-Profile</i>	$(z-d)/L$ is within the unstable window set for the site
<i>COTAG</i>	COnditional Time Average Gradient system
d	Zero-plane displacement height (approximated as $0.65 * h_{canopy}$)
<i>DELTA</i> ®	DEnuder for Long-Term Atmospheric sampling
F	Flux, flow of a property per unit area (conventionally $F > 0$ in case of emission; $F < 0$ in case of deposition)
h_{canopy}	Height of the canopy above ground level
<i>ICOS</i>	Integrated Carbon Observation System – Research infrastructure for standardized greenhouse gas measurements throughout Europe
κ	von Kármán's constant (~0.41)
<i>KT04</i>	VMM code for the COTAG site in Kalmthout
L	(Monin-)Obukhov length, a measure of atmospheric stability
<i>LOD</i>	Limit of detection
<i>MA12</i>	VMM code for the COTAG site in Maasmechelen (ICOS site)
NH_3	Ammonia
R_a	Aerodynamic resistance
R_b	Laminar boundary layer resistance
R_c	Canopy resistance
t	Time of measurement period
u^*	Friction velocity, a measure of turbulent surface stress
v_d	Dry deposition velocity
v_{max}	Theoretical maximum dry deposition velocity
z	Measurement height above ground level of the sonic anemometer
$(z-d)/L$	Atmospheric stability parameter

1 Introduction

This study is funded by public procurement contract *VMM/LUC/2020/NH₃-depositie*¹ and *VMM/LUC/2022/COTAG-metingen*² and was carried out by the UK Centre for Ecology & Hydrology (UKCEH) on behalf of and in cooperation with Flanders Environment Agency (*Vlaamse Milieumaatschappij*, VMM).

Monitoring ambient air quality in Flanders is one of the tasks of VMM. In recent years the importance of ammonia (NH₃) as a regional pollutant has been recognised due to its role in aerosol formation and the eutrophication and acidification of ecosystems. The large emissions of NH₃ from anthropogenic activities in this part of Europe strongly contribute to the atmospheric nitrogen deposition to many of the natural ecosystem sites. NH₃ concentrations are currently monitored by VMM with diffusive (passive) samplers and real-time miniDOAS monitors.

In addition to ambient NH₃ concentrations, it is important to quantify the flux of NH₃ between the atmosphere and the Earth's surface, in order to assess the contribution of NH₃ to nitrogen deposition at sensitive ecosystems. In Flanders, the net flux of NH₃ is to the surface and it is referred to as dry deposition. According to measurements and model results, dry deposition of NH₃ is a meaningful contribution to the high atmospheric nitrogen deposition in the region (Neiryneck et al., 2005, 2007; Rutledge-Jonker et al., 2023). However, to our knowledge there are no recent direct flux measurements of NH₃ in Flanders.

Therefore, the purpose of this study was to measure the NH₃ flux at two background locations in nature reserves in Flanders. The project involved the implementation of long-term autonomous measurements as part of a routine monitoring network. Measuring NH₃ fluxes is not straightforward because of the high reactivity of this gas, and measurements at high temporal resolution generally require complex and labour-intensive setups. The aim of this study was to measure the net flux of NH₃ at a low temporal resolution (4 weeks).

The methodology used is known as the COnditional Time Average Gradient (COTAG) system. This is based on the aerodynamic flux gradient method and allows net NH₃ flux measurements with a time resolution of typically 2 weeks to a month. To calculate the net flux the method requires information on the vertical concentration gradient and the transfer rate (eddy diffusivity) across this gradient. Hence, the main measurements in a COTAG system are the concentration gradient of NH₃, determined with coated glass denuders at two heights, and the atmospheric turbulence, measured with an ultra-sonic anemometer.

The measurements were carried out at:

- Kalmthout (Kalmthoutse Heide): purple moor grassland surrounded by dry heathland;
- Maasmechelen (Mechelse Heide): dry heathland.

In this study UKCEH was responsible for:

¹ *Levering en installatie van 2 meetopstellingen voor ammoniakdepositie en analyse van 1 meetjaar*

² *Onderzoek naar de droge depositie van ammoniak door middel van COTAG-metingen*

- Analysing the suitability of potential measurement locations proposed by VMM;
- Building and installing the COTAG systems at two locations;
- Preparing, extracting and analysing the denuders.
- Supporting the measurements, analysing, interpreting and reporting the results.

VMM was responsible for:

- Proposing and documenting potential measurement locations;
- Installing the masts, sonic anemometers and power supply;
- Operating and maintaining the COTAG systems and replacing the denuders in the field.

This report is the study of the results of forty-one 4-weekly periods of NH₃ flux measurements (from 09/11/2021 to 31/12/2024).

2 COTAG system

2.1 Principle of operation

The COTAG is based on the aerodynamic flux gradient method (Monteith, 2013), which requires a vertical profile of gas concentration and information on the eddy diffusivity across the vertical concentration gradient to calculate the flux. In the system the NH₃ concentration gradient is measured at two heights with 14 glass denuders (which work on the principle of chemical capture of a substance to measure gas concentration) and the atmospheric turbulence is determined via a sonic anemometer.

Over the period of a day, atmospheric conditions can range from highly stable, where the vertical gradients of ambient concentration are enhanced due to very small diffusivity, to highly unstable conditions, in which concentration gradients are small due to the intense turbulent activity and mixing in the surface layer. As a result, empirical corrections are required to account for the different atmospheric stabilities, as without, in the case of highly stable conditions an uncorrected concentration gradient would lead to an overestimation of the flux.

As the COTAG only measures gas concentration gradients at a low temporal resolution (e.g., 4 weeks in this study), the system overcomes corrections required by sampling a concentration profile conditionally, using micrometeorological variables from the preceding 30 minutes for a carefully defined range of stability. This therefore excludes periods where corrections for the flux are large. The system obtains the micrometeorological variables required to determine the atmospheric stability from a sonic anemometer using the eddy covariance method (Foken, 2008). Averages over a period of 30 minutes are used as this time is long enough to sample the full spectrum of turbulent eddies contributing to the flux, and short enough to provide reasonably constant surface and atmosphere conditions.

The Monin-Obukhov length L (Garrat, 1994), defined in the following equation, is often chosen as a parameter to assess the stability condition of the atmosphere:

$$L = \frac{-u_*^3 T_v}{\kappa g Q_{v0}} \quad (1)$$

Where κ is von Kármán's constant, u_* is the friction velocity (a measure of turbulent surface stress), g is gravitational acceleration, T_v is virtual temperature (corresponding to sonic temperature), and Q_{v0} is a kinematic virtual temperature flux at the surface (corresponding to H , sensible heat flux).

Based on the Monin-Obukhov length L , the dimensionless variable z/L (where z is measurement height above the surface of the sonic) is used in the COTAG system as a stability parameter, with $z/L = 0$ for statically neutral stability, positive in stable and negative in unstable stratification.

At each measurement site the COTAG operates within a site-specific window of neutrality that is initially set and then revised with time according to the micrometeorology of each site.

The measurement system is programmed to sample only when the fetch is unaffected by obstacles, as defined by the operator through the inspection of the surface topography and land use within the distance of interest at the measurement site. The system samples concentrations of the pollutant in the air when atmospheric predefined conditions of stability are met.

2.2 The aerodynamic flux gradient method

In the aerodynamic gradient theory the vertical flux of a scalar χ (in this case NH_3 concentration) is determined from its vertical concentration gradient and the eddy diffusivity coefficient K_χ (Foken, 2008; Kaimal and Finnigan, 1994), which is a function of the friction velocity (u_*), the measurement height (z) and the Monin-Obukhov length L that provides a measure of the atmospheric stability.

$$F_\chi = -K_\chi(u_*, z, L) \frac{\partial \chi}{\partial z} \quad (2)$$

The Aerodynamic Gradient Method (AGM) assumes that heat and mass are transported in similar ways within the surface atmospheric layer, where fluxes are considered constant with height (Foken, 2008).

In practical terms, the flux gradient is calculated as the integral form between two measurement heights, z_1 and z_2 , above the ground and in this study is expressed as (Flechar, 1998):

$$F = -\kappa u_* \frac{\Delta \chi}{\ln\left(\frac{z_2 - d}{z_1 - d}\right) - \psi_H\left(\frac{z_2 - d}{L}\right) + \psi_H\left(\frac{z_1 - d}{L}\right)} \quad (3)$$

Where κ is the von Karman's constant ($\kappa = 0.41$), d is the zero-plane displacement height (in this study $d = 0.65 * h_{canopy}$) and ψ_H is the integrated stability correction function for heat that accounts for deviation from the log-linear profile in non-neutral conditions. There are several expressions for ψ_H in literature, in this study we use the formulation as in Dyer and Hicks (1970) and Webb (1970) for the unstable and stable atmosphere, respectively. Conventionally, a positive flux is associated with emission and a negative flux with deposition of the scalar component.

The stability corrections applied to the flux are a function of $(z-d)/L$: the correction for non-logarithmic profiles is small in the fully forced convection region (values of $(z-d)/L$ around 0), whereas it increases more rapidly as the atmospheric conditions move towards free convection ($(z-d)/L < 0$) or lack of convection ($(z-d)/L > 0$). To minimise the magnitude of the correction applied to the flux it is therefore necessary to set the $(z-d)/L$ values for the conditional sampling window close to the fully forced convection region. The choice of the window of neutrality is a compromise to maximise the time of data acquisition and to keep close to the atmospheric neutrality.

2.3 Denuders

In terms of sampling logic, the 14 sensors are sub-divided into 3 sets (two of 6 and one of 2 samplers), one of which is sampling at any one time. Of the sets of 6, three of each will be placed at two different heights of a mast, in the ‘top box’ and ‘bottom box’ (Figure 1), providing the near-neutral/stable profile (A) and the unstable profile (B). All denuder samplers are connected by means of plastic tubes to gas flow meters and eventually to an air pump. All electronic components are connected to a data logger, which is programmed to store and average the wind and temperature data, as well as to switch on or off the pump connected to the individual set of denuders, making the gas capture possible only in the desired conditions, i.e. excluding bad fetch conditions (low wind speed and wind direction from flow-disturbed areas). Of the set of two samplers, one is placed on the mast at the higher height and the other one to the lower height to be operated during periods of extreme micrometeorological conditions, when the flux is not measured (“off” denuder). A summary of the sampling classes used in the COTAG sampling is provided in Table 1.

Table 1: Summary of the COTAG sampling classes.

Denuders sets	Measurement	Description
“off” denuder	Concentration only	Wind speed is too low or wind direction is discarded due to an obstruction at the site.
“off” denuder	Concentration only	Atmosphere is too unstable or too stable: $(z-d)/L$ is out with the selected stability windows for the site
A-Profile	Flux	Stability parameter $(z-d)/L$ is within the stable/near-neutral window set for the site
B-Profile	Flux	Stability parameter $(z-d)/L$ is within the unstable window set for the site

The denuders for chemical detection utilize the DELTA[®] approach (DEnuder for Long-Term Atmospheric sampling, <https://www.ceh.ac.uk/services/delta-active-sampler-system>) (Tang et al., 2009) of active sampling using a sample train consisting of a series of coated denuders to collect acid gases, inorganic aerosols and NH₃. The DELTA is optimized to sample at a low air flow rate (0.3 - 0.4 litres per minute) allowing samples to be exposed over monthly periods (further details can be found in Tang et al. (2018)). In this study only NH₃ was sampled, so that the sampling trains (Figure 2) consisted of a short glass inlet (2.3 cm, to develop laminar flow), plus short denuder (15 cm) coated with citric acid to remove gaseous NH₃ from the air stream, followed by a glass outlet (not coated), to protect coated denuder from contamination during sample changes.

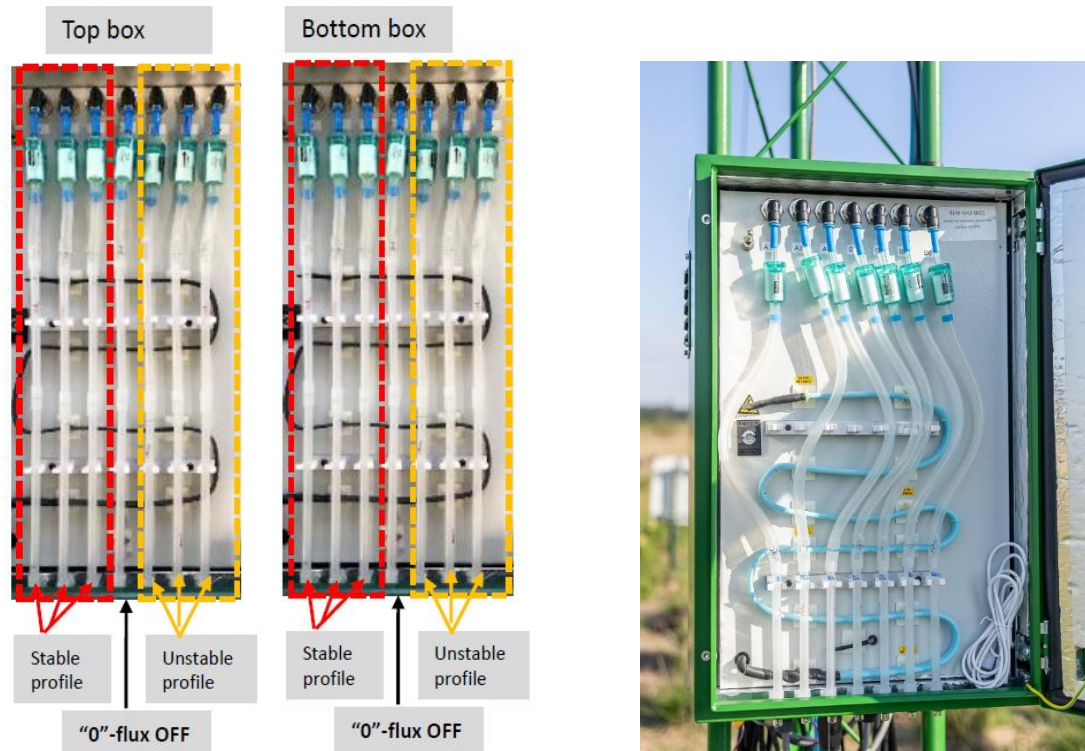


Figure 1: Sampling trains assembly in the COTAG system boxes ("0"-flux OFF - sampling train for when no flux measurements are taken). The near neutral/stable profile is also referred to as A-profile and the unstable profile as B-profile.

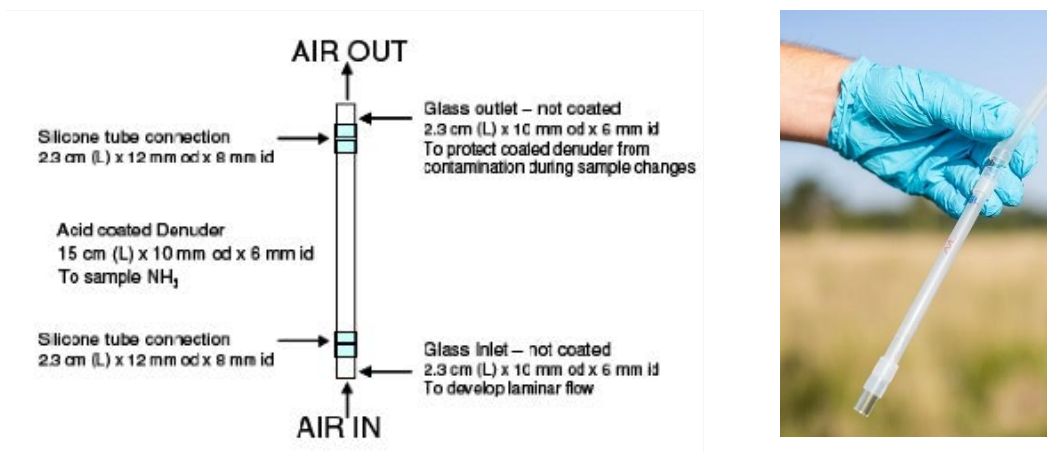


Figure 2: Schematic of the sampling train used for collecting gaseous NH_3 in the COTAG system.

For a thorough description of all components, refer to the relative sections in the manual.

2.4 Analytical methodology

2.4.1 Preparation of samples and analysis

The denuders were prepared and extracted using the Standard Operating Procedure (SOP) described in the protocol developed for the COTAG system during the EU FP 6 NitroEurope project. The chemical analysis was based on the same analytical procedure used by the DELTA[®] method which uses citric acid coated denuders. This SOP used for analysis follows the accredited analytical method by the United Kingdom Accreditation Service (UKAS) at our laboratory at UKCEH Lancaster. The UKCEH Edinburgh laboratory itself, however, is not UKAS accredited, though it developed the analytical procedure used in Lancaster.

Fourteen citric acid coated denuders (15 cm length x 6 mm inner diameter) were used in the operation of a COTAG system at any one time. After exposure samples were returned to the UKCEH Edinburgh laboratory where they were placed in a cold store ($4^{\circ}\text{C} \pm 2^{\circ}\text{C}$) until analysed. Samples were extracted using ultra-pure deionised water ($>18 \text{ M}\Omega \text{ cm}$). The extracted fluid was analysed by colorimetric technique, based on detection of a colour change response selective for ammonium, using a SEAL-AA3 instrument (<https://www.seal-analytical.com>). The detection limit of this instrument is quoted as $0.03 \text{ mg NH}_4^+\text{-N L}^{-1}$.

As part of the analysis method, calibrations and quality control samples were run as well as background lab blanks and transport blanks to remove any error from contamination collected during storage or transit. The calibration range used is $0 - 10 \text{ mg L}^{-1} \text{ NH}_4\text{-N}$ and the quality controls QCs are 0.05, 0.5, 2, 5 and $9 \text{ mg L}^{-1} \text{ NH}_4\text{-N}$. As such, the detection limit for NH_3 measurement using DELTA denuders was determined as $3 \times$ standard deviation of a series of extracted lab blanks ($\mu\text{g NH}_3$) / volume of air sampled ($\sim 15 \text{ m}^3$ @ flow rate of 0.35 L min^{-1}). For the COTAG this leads to a limit of detection (LOD) of $0.02 \mu\text{g NH}_3 \text{ m}^{-3}$ for monthly sampling, and a measurement method uncertainty of 5%: lab tests showed a 99% recovery for all QC levels except for the lower concentration where the recovery was between 95% and 99%.

Since each set of COTAG denuders only samples for a fraction of the time, the actual LOD increases accordingly as sampling volume decreases. As part of quality assurance checks, samples were evaluated for their condition prior to analysis and any field comment was used to flag results appropriately.

2.5 Quality control of NH_3 concentrations: removal of outliers

As part of the quality control processes the NH_3 concentrations were examined and unreliable data points were rejected following the steps:

- when technical issues on the field or in the lab were highlighted;
- when the coefficient of variation (CV) of the NH_3 concentration replicates was $>15\%$; in this case the data point that caused the CV to be $>15\%$ was considered an outlier.

2.6 Limitations

There are three main limitations of the COTAG methodology that can lead to underestimation or overestimation of the flux:

- the delay in determining the stability class;
- the long-term sampling ignoring the “cross-term”;
- the conditional sampling ignoring fluxes in off- mode.

In addition, uncertainty in the displacement value d contributes to the uncertainty of the flux.

2.6.1 Delay in determining the stability class

The stability class that defines the set of denuders through which the air is sampled is selected based on atmospheric stability measurements made in the 30 minutes preceding the sampling.

Famulari et al.(2010) and Rutledge-Jonker et al.(2023) showed that this delay did not affect the flux so no delay-related corrections were made to the flux in this study.

2.6.2 Long-term sampling ignoring the “cross-term”

The COTAG flux is the product of the “4-weekly” average concentration difference $\Delta\chi$ and the “4-weekly” average F^* , calculated from the atmospheric variables like in expression (3). The result differs from a flux obtained by multiplying the two terms before averaging them. In an ideal case, we would have 30-minute fluxes and then average them over 4 weeks. The difference between the two methods is referred to as “cross-term” (Famulari et al., 2010).

Although Famulari et al.(2010) showed a negligible effect of the cross-term on the flux, Rutledge-Jonker et al.(2023) quantified the effect with results varying between 2 and 15% depending on the stability and month of the year. They showed a seasonality of the impact reflected in the a_{cross} coefficient derived by comparing the simulated flux obtained with the two averaging approaches (long-term averaging like in the COTAG and monthly averaging of the 30-min fluxes). The corrected flux F_{corr} can then be estimated from the measured flux (F_{COTAG}) as:

$$F_{corr} = \frac{F_{COTAG}}{a_{cross}} \quad (4)$$

where a_{cross} was derived by monthly values in Rutledge-Jonker et al. (2023) and adapted to a 4-weekly sampling period (Table 2). It must be noted that in this study the cross-term correction was applied to the gap-filled deposition calculation and not to the flux calculation in Section 4.4.

Table 2: Seasonal values of the cross-term correction across for the neutral (A) and unstable (B) profiles.

End of sampling date – 13 periods in a year	$a_{\text{cross_neu}}$	$a_{\text{cross_uns}}$
01/02	1.07	1.04
01/03	1.09	1.04
29/03	1.13	1.03
26/04	1.14	1.06
24/05	1.14	1.05
21/06	1.17	1.12
19/07	1.16	1.09
16/08	1.14	1.07
13/09	1.14	1.07
12/10	1.12	1.02
07/11	1.09	1.02
07/12	1.07	1.01
03/01	1.08	0.99

2.6.3 Conditional sampling ignoring fluxes in off-mode

The conditional sampling leads to ignoring fluxes when the system is in off-mode, underestimating the total deposition, depending on how frequently the off-mode occurs. This is perhaps the COTAG limitation with the greatest impact on the quantification of dry deposition.

To account for the lack of flux measurements during the COTAG off-mode, Rutledge-Jonker et al. (2023) proposed a gap-filling method based on a study comparing simulated fluxes for the different stability classes at several of their COTAG background sites. They showed that the flux in one stability class correlated well with the flux in the neighbouring stability class and they suggested a gap-filling approach described in Section 4.5.

Note that the methodology adopted in this report to calculate NH_3 deposition is an updated and revised version of the one used in Di Marco et al. (2024).

2.6.4 Zero-plane displacement height

An important contribution to the systematic uncertainty in COTAG-derived deposition estimates is due to the (zero-plane) displacement height d . The displacement height is the notional displacement of the Earth's surface due to the effect of vegetation on turbulence (Rutledge-Jonker et al., 2023). It is the height at which zero mean wind speed is achieved as a result of flow obstacles such as vegetation. In other words, it is the distance above the ground at which a non-vegetated surface should be placed to provide a logarithmic wind field equal to the observed one.

Determining d can be difficult due to the heterogeneous and slightly undulating landscape and to seasonal changes in vegetation height (Rutledge-Jonker et al., 2023). As a rule of thumb d is generally estimated as a proportion of the canopy height (h_{canopy}):

$$d = 0.65 \cdot h_{\text{canopy}} \quad (5)$$

This approach was used in the COTAG flux calculation, assuming d as a constant value throughout the year, but it was decided to carry out wind profile measurements. In this way we can derive a local, specific value of d and the potential seasonal variation of it. This study includes results for both COTAG sites as described in Section 4.6.

3 Sites description

3.1 Criteria for site selection

The site selection process is described in a previous report (Di Marco et al., 2022). The chosen sites had to fulfil some technical criteria required by the measurement technique:

- homogeneity of land use;
- absence of NH₃ sources in the vicinity;
- feasibility of the set-up and availability of mains power;

and some more general criteria related to the long-term sustainability of the measurements:

- vegetation type (natural low vegetation);
- site management and ownership (stable management in the long term);
- location in two different regions or provinces of Flanders (maximise the information on spatial variability).

Based on online meetings and documentation (maps, pictures, wind data) provided by VMM, UKCEH agreed to select the proposed sites at the Mechelse Heide (MA12) and Kalmthoutse Heide (KT04). The two measurement sites are indicated on a map of modelled annual NH₃ concentrations in 2021 in Flanders in Figure 3.

Due to travel restrictions in relation to SARS-CoV-2, it was not feasible for UKCEH to visit these sites before installing the COTAG instruments in October 2021.

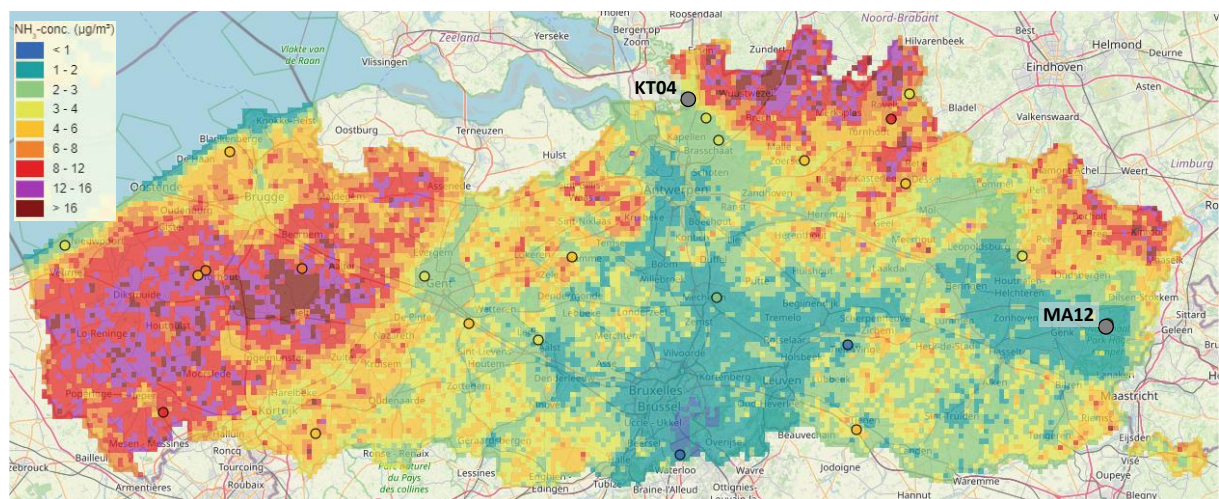


Figure 3: Map of the modelled mean annual NH₃ in 2022 (VLOPS24, 1x1 km² grid) and the locations of the sites Kalmthoutse Heide (KT04) and Mechelse Heide (MA12).

3.2 Maasmechelen (Mechelse Heide)

The current NH₃ monitoring site of VMM in Maasmechelen (MA12) is in the nature reserve 'Mechelse Heide'.

This site has been set up by the University of Antwerp (UA) in the framework of the ICOS project (Integrated Carbon Observation System; <https://www.icos-belgium.be>). Greenhouse gas fluxes and meteorological variables have been measured since 2016. An underground technical cabin was built near the sand road (Figure 5). The roof of the building is ~50 cm above the soil level. The site is a large open dry heathland area with some trees scattered around at 50 m N and 100 m E of the COTAG measurement point and some ground micro-relief, including holes of ~1 m depth. The location of the COTAG in relation to the ICOS mast and the cabin is shown in Figure 4.

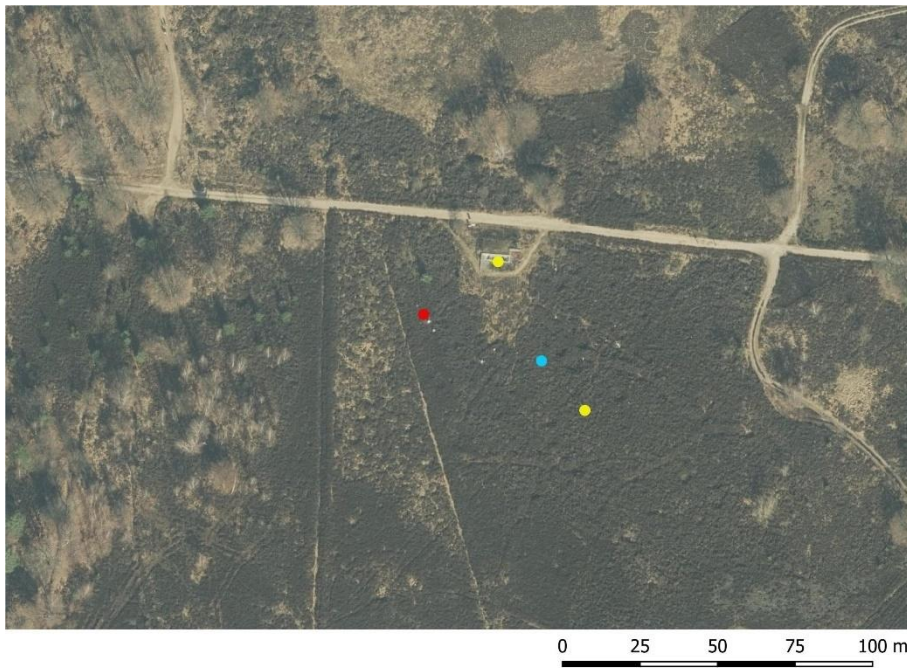


Figure 4: Set-up location of equipment at the Mechelse Heide site: VMM NH_3 passive sampling in red, ICOS facilities in yellow and COTAG location in blue.



Figure 5: ICOS flux tower (left) and underground technical building (right).

VMM have been measuring ambient concentrations of NH_3 , NO_2 and wet deposition at site MA12 since 2018 (Figure 6 left). As Maasmechelen is part of the ICOS network,

continuous eddy covariance measurements of CO₂ have been made for the past few years alongside measurements of wind speed, wind direction, temperature and turbulence. Data from this network for the year 2020 were used to support an initial assessment of the atmospheric stability for this study.



Figure 6: Left photo: VMM monitoring instruments (wet-only sampler, precipitation volume, NH₃ and NO₂ passive samplers). Right photo: View of the heathland to the SW from the COTAG location (April 2021).

3.3 Kalmthout (Kalmthoutse Heide)

Grenspark Kalmthoutse Heide is a large nature reserve situated on both sides of the Belgian-Dutch border. The location of the COTAG is in a large open dry heathland with purple moor grass (*Molinia caerulea*; Figure 7).



Figure 7: SW view from the COTAG site in Kalmthout.

VMM has no long-term air quality monitoring in the area, but NH₃ measurements have periodically been carried out between 2015 and 2017 at several sites in the reserve. Based on the availability of mains power, on the presence of flat terrain and on the feasibility of digging soil, the preferential site was in a flat parcel of *Molinia* grassland,

south of the Korte Heuvelstraat (Figure 8). This site is about 100 m from the NH₃ measurement site KT04 used in 2015-2016 and 2017.



Figure 8: Set-up location of equipment at the Kalmthoutse Heide site: former VMM NH₃ passive sampling site (KT04) in red, existing facilities in yellow and COTAG site in blue.

The area is occasionally used for grazing animals (sheep) during the growing season, typically in May-July and October. The COTAG parcel is relatively large (between Korte Heuvelstraat north and the lake 'Putse Moer' south), so recorded grazing in this parcel does not necessarily mean that sheep were present in the direct neighbourhood of the COTAG.

3.4 COTAG system set up at VMM sites

The technical specifications of the COTAG can be found in the manual.

The COTAG systems were installed in October 2021 at the two sites (refer to section 3.3) and have been sampling since 9 November 2021. The main components of the COTAG systems at the sites are (Figure 9):

- A triangular open mast (4 m high, sides of 30 cm) on a baseplate (50 x 50 cm²) to which two sampling boxes (60 x 40 x 26 cm³) are attached;
- A pole (~2.5 m high) with an ultra-sonic anemometer (Gill Windmaster 1590-PK-020/W);
- A box for power supply, VMM datalogger (SAM Lite) and modem.

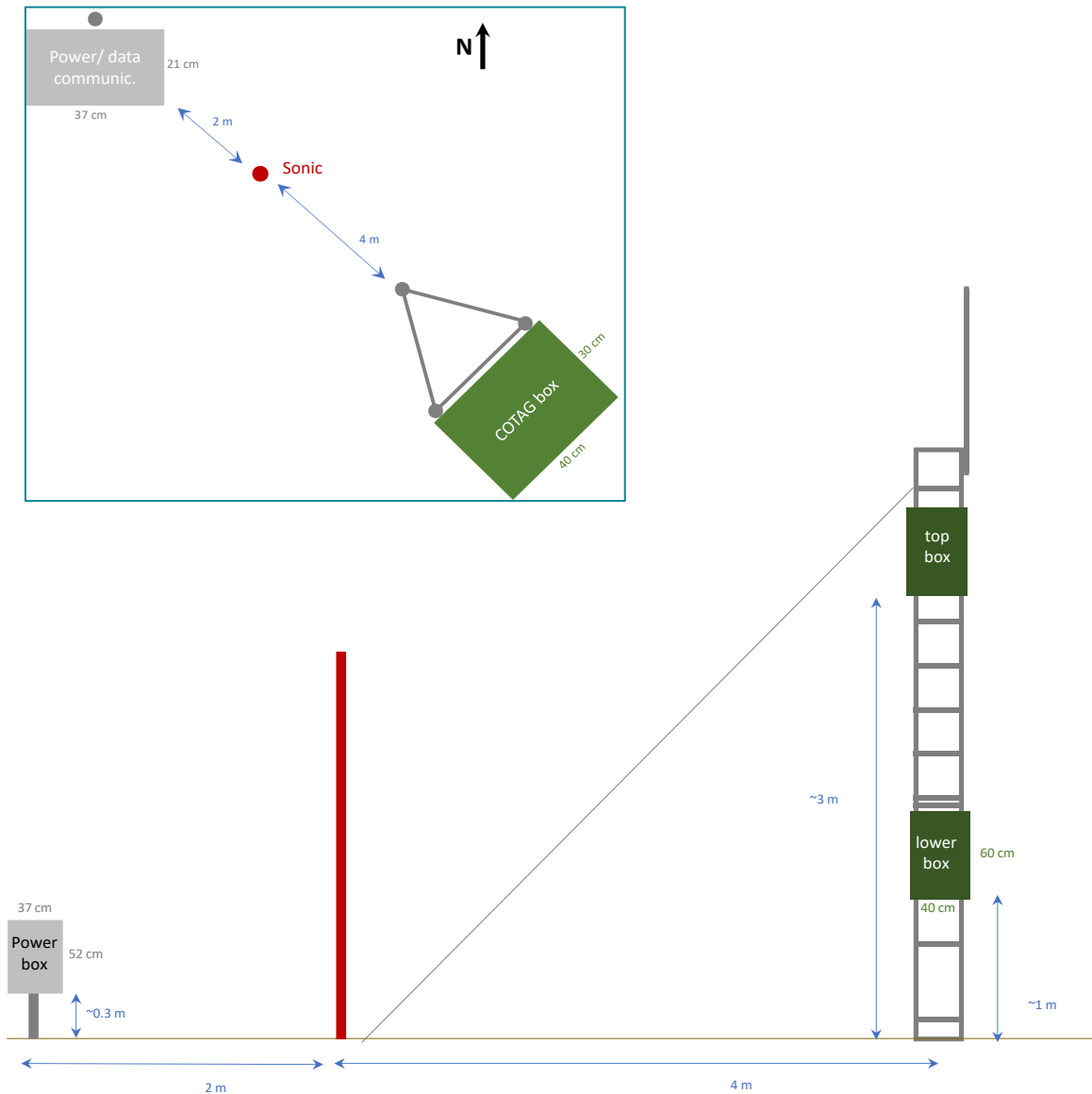


Figure 9: Plan of VMM COTAG: view from above and side-view.

The horizontal distance between the sonic pole and the mast is about 4 m. At both sites, the power box, sonic and mast are on a NW-SE line to avoid turbulence around the sonic and the sampling boxes in the main SW and NE wind sectors.

The mast and pole are anchored to the soil with wires and metal rods (1.5 m). On top of the mast is a lightning rod (1.25 m) connected by a copper wire to a separate grounding. To protect the sonic, one of the base screws is connected by a copper wire to the main grounding of the power box.

The two setups are identical, except for the colour of the mast and COTAG sampling boxes:

- Kalmthout (KT04): green - RAL 6002 (Figure 10);
- Maasmechelen (MA12): light grey - RAL 7035 (Figure 11).



Figure 10: COTAG installed at Kalmthout.



Figure 11: COTAG installed at Maasmechelen.

A summary of the settings used at the two sites for measurements and canopy heights, stability window and discarded wind sector is shown in Table 3. Note: the stability windows changed in July 2023.

Table 3: Summary of measurement heights, wind and stability settings in use for conditional sampling at the selected sites.

	MAASMECHELEN (MA12)	KALMTHOUT (KT04)
Canopy height (cm)	90	80
Height of top box (cm)	306	308
Height of bottom box (cm)	109	98
Sonic height (cm)	255	256
Discarded wind sector (°N)	322-8; 151-158	136-156
Wind cut-off (m/s)	0.8	0.8
Stable/near neutral profile-A	-0.02 < (z-d)/L ≤ 0.02 -0.03 < (z-d)/L ≤ 0.03*	-0.02 < (z-d)/L ≤ 0.02 -0.03 < (z-d)/L ≤ 0.03*
Unstable profile-B	-0.1 < (z-d)/L ≤ -0.02 -0.14 < (z-d)/L ≤ -0.03*	-0.1 < (z-d)/L ≤ -0.02 -0.14 < (z-d)/L ≤ -0.03*

* Values in use after 18/07/2023

4 Results

In the following sections the terms “monthly” and “4-weekly” are used interchangeably.

4.1 Wind roses

The main wind directions for both Maasmechelen and Kalmthout were SW and NE as shown in Figure 12 through to Figure 13. The wind speed for these sectors is mainly larger than 2 m s^{-1} , providing a well-mixed surface atmospheric layer. As mentioned before, for the conditional sampling of the COTAG there is a need to exclude situations when the atmosphere is highly stable, which often includes night-time or more generally periods with very low wind speeds. At very low wind speed there is no turbulence to drive fluxes and the measurement of fluxes, stability and wind direction becomes highly uncertain. For this reason, a wind speed cut off was applied to the sampling program of the COTAG: when the wind speed was lower than 0.8 m s^{-1} the system did not measure fluxes. Bearing in mind the uncertainty in the wind direction, at Maasmechelen low wind speeds seemed to be associated mostly with the W-NW sector, which is prevalent in the spring/summer months (Di Marco et al., 2024), resulting in low data capture (refer to Section 4.2 for further details). The wind rose measured by the COTAG system between Nov 2021 and Dec 2024 was in good agreement with the wind rose measured by the ICOS instruments (Figure 12). At Kalmthout, the wind seasonality was very similar, with stronger winds from SW during the winter months and lighter winds with less constant direction in the spring and summer as shown in a previous report (Di Marco et al., 2024, Figure 13).

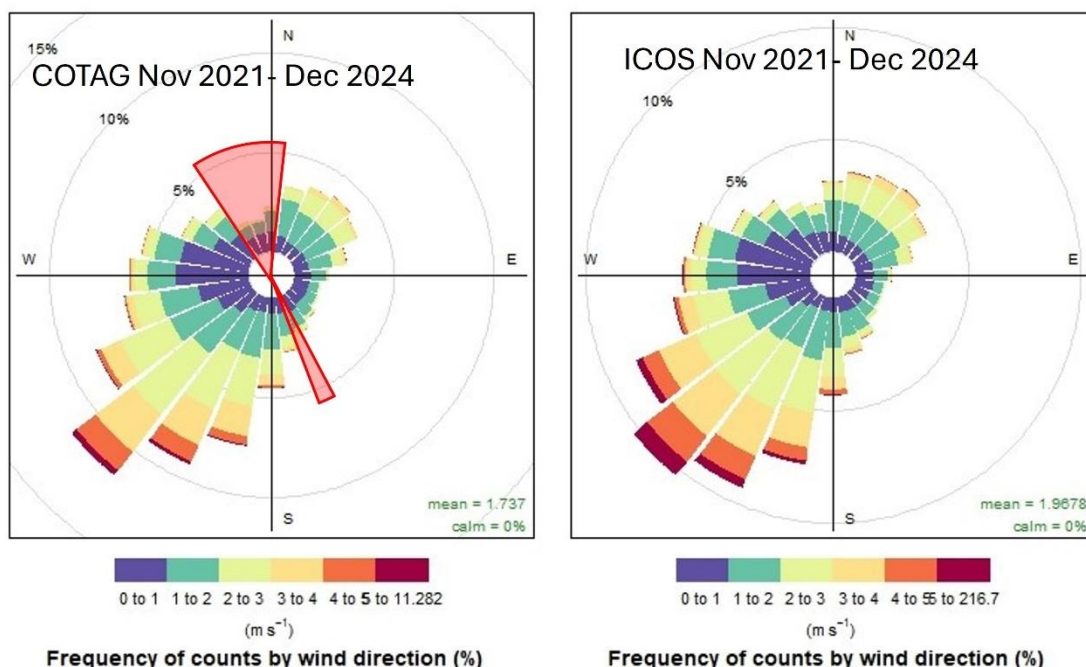


Figure 12: Wind roses at Maasmechelen. On the left is the wind rose measured by the COTAG system and on the right the wind rose from the ICOS data for the period publicly available. The red shaded area is the rejected wind sector. Values on the radius indicate the percentage of occurrence. Wind speed is colour coded as in the legend.

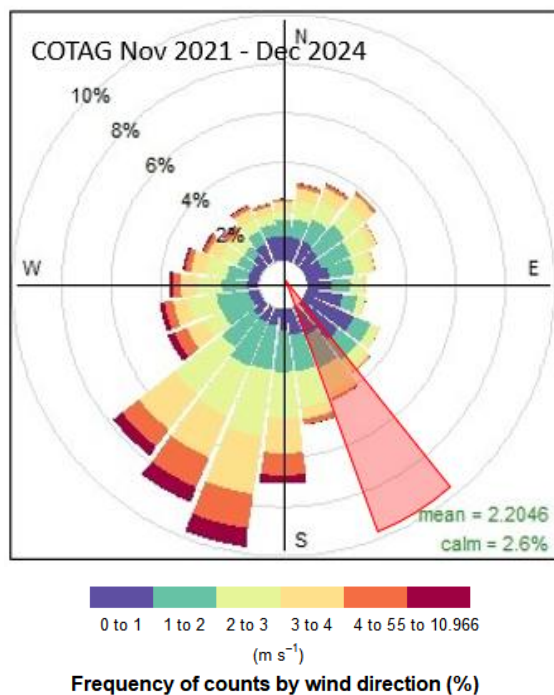


Figure 13: Overall (November 2021 – December 2024) wind rose with wind speed classes measured by the COTAG system at Kalmthout. The orange shaded area is the discarded wind sector. Values on the radius indicate the relative contribution of each wind sector in %.

4.2 Data capture

The 4-weekly data capture divided by sampling classes for the period November 2021 to December 2024 is shown in Figure 14 and Figure 15 for Maasmechelen and Kalmthout, respectively. The coloured areas (red + green) represent the time when the COTAG measured fluxes, and the grey shades represent the time when no flux was measured but air was instead sampled through the “off” denuders to measure concentrations. For the first two years of measurements, the flux data capture ranged between 40% and 60% during the winter months. For most of the time during the spring and summer periods at both sites the capture was less than 40%.

After a study on the effect of variation of the stability classes on the capture (Di Marco et al., 2024), it was decided to relax the windows in July 2023 to improve the data capture (Table 1). The values of the new windows were calculated using the same $1/L$ value as for the Dutch COTAGs, adjusted for the sonic anemometer and displacement heights used for the Belgian COTAGs. Since then, the data capture increased in the last year of measurements, ranging between 50% and 70% in winter and 30% and 50% in summer.

The effect of the change in stability windows introduced in July 2023 is shown in Table 4. The overall capture increased at both sites due to the relaxation of the stability windows. The stable/near-neutral profile-A (green shade) was prevalent during the cold months (November to February) when the atmosphere is generally more stable, while the occurrence of the unstable profile-B (red shade) increased during the warmer months from March until August/September when there was greater turbulence. At

Maasmechelen the portion of time when the wind speed was below the cut-off or the wind direction was in the excluded sector (light grey shade) increased from 20-30% in the winter months to up to 40% in the summer months (Figure 14). At Kalmthout wind speed and wind direction were out of the desired range for 20-30% of the time for most months (Figure 15). At both sites the portion of time when atmospheric conditions were too stable despite a wind speed above the cut off (dark grey shade) was between 10% and 30% with greater occurrences in winter. Conversely, conditions were too unstable (pattern shade) for 10-20% of the time during the summer months and there was almost no occurrence of this class in winter. The frequency of down time due to MFC calibrations or power cuts varied (black shaded area), with Maasmechelen having a down-time of less than 1% on average. Kalmthout on the other hand had more power cuts resulting in up to 30% down-time in June 2022 (Figure 15). Overall, the data capture for NH₃ concentrations ranged between 96% and 100% in Maasmechelen and between 72% and 100% in Kalmthout (November 2021 to December 2024). The initial power issue at Kalmthout was addressed and did not represent itself in 2023 nor 2024.

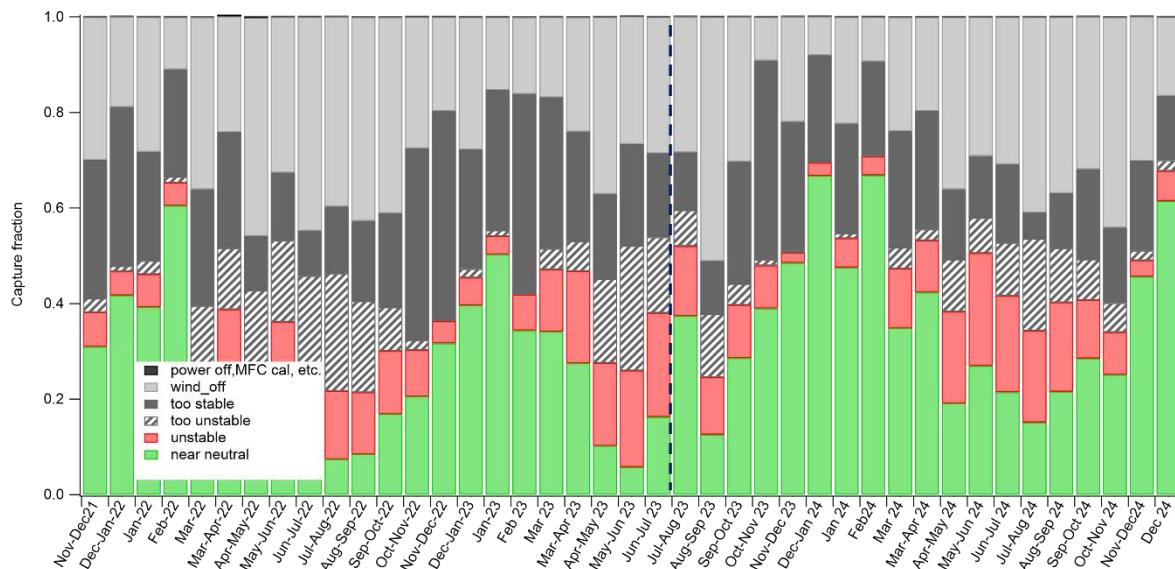


Figure 14: “4-weekly” COTAG data capture at Maasmechelen from November 2021 until December 2024. The black dashed line indicates the change in stability windows.

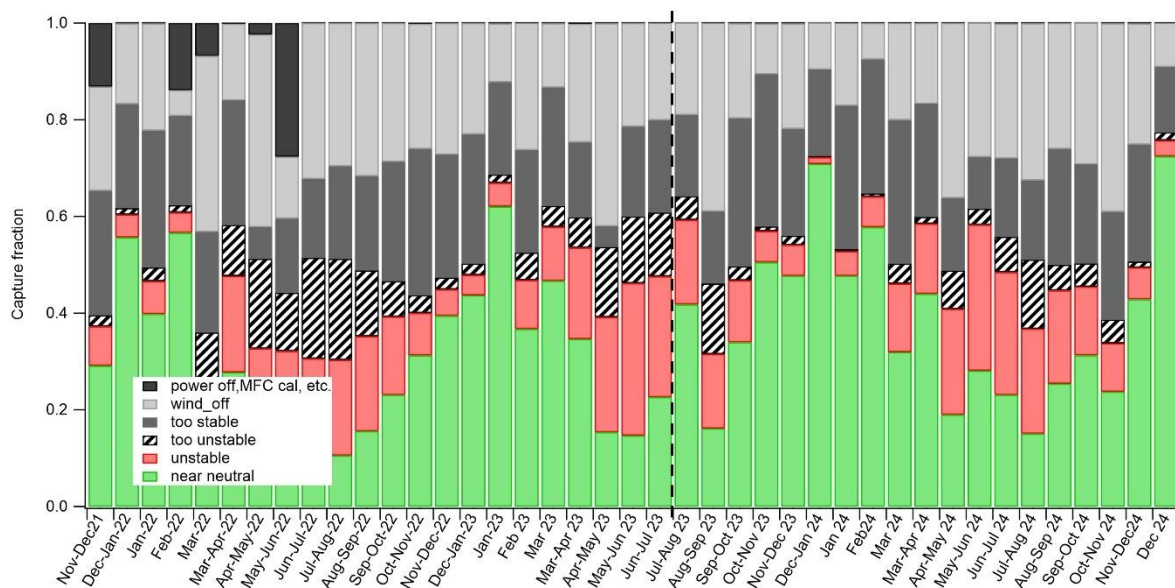


Figure 15: “4-weekly” COTAG data capture at Kalmthout from November 2021 until December 2024. The black dashed line indicates the change in stability windows.

Table 4: Statistics of data capture at Maasmechelen and Kalmthout before changing the stability windows (November 21-July 23) and after the change in stability windows (July 23-December 24).

Averaging period	Maasmechelen						Kalmthout					
	Nov 2021-July 2023			July 2023-Dec2024			Nov 2021-July 2023			Jul 2023-Dec2024		
	av.	min	max	av.	min	max	av.	min	max	av.	min	max
Power off	0%	0%	0%	0%	0%	0%	3%	0%	28%	0%	0%	0%
Wind off	29%	11%	46%	27%	8%	51%	24%	5%	42%	21%	8%	39%
Too stable	24%	10%	44%	19%	6%	42%	20%	4%	30%	22%	11%	32%
Too unstable	10%	0%	26%	6%	0%	19%	9%	1%	21%	4%	0%	15%
Unstable/ profile B	12%	4%	22%	11%	2%	24%	14%	4%	32%	14%	1%	30%
Near-neutral/ profile A	24%	5%	61%	37%	13%	67%	30%	10%	62%	39%	15%	72%

For the flux measurements over the period November 2021 to December 2024 at Maasmechelen the overall capture (intended as the proportion of flux measurements included in the stability window) was 57%, of which 42% in the near-neutral/stable stability class and 15% in the unstable one (Figure 16). At Kalmthout the overall capture was 66% with 50% in the near-neutral/stable profile and 16% in the unstable one (Figure 17).

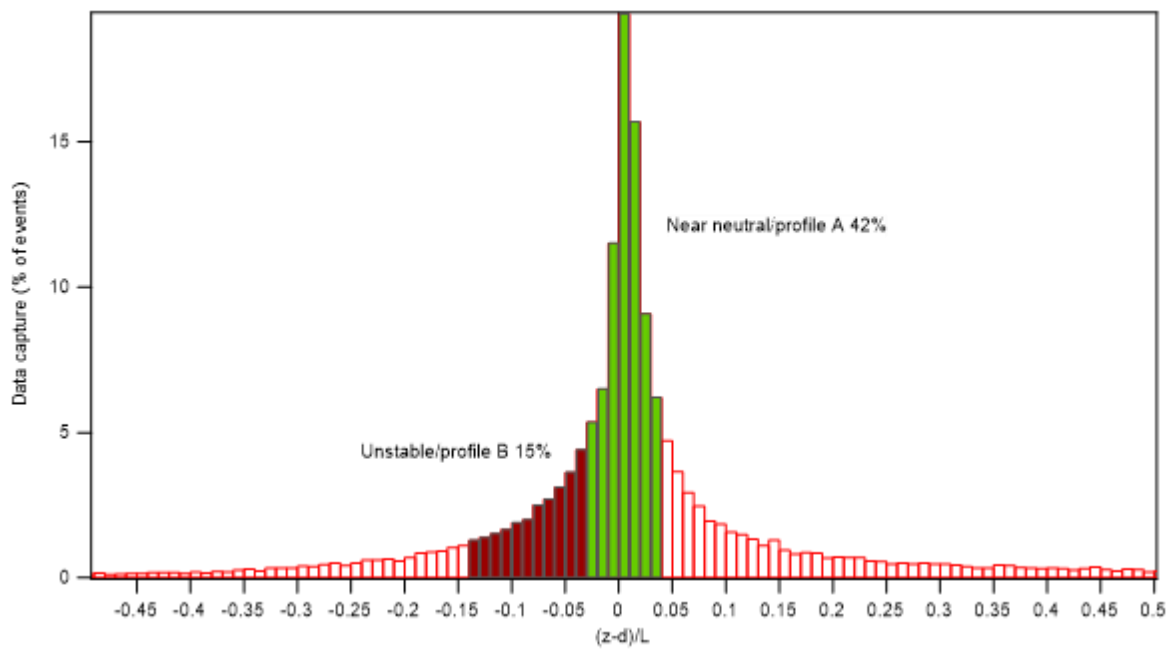


Figure 16: Distribution of the stability parameter for the period November 2021-December 2024 at Maasmechelen. The coloured shades show the two COTAG profiles capture. Data presented are filtered by wind speed cut off and wind sector.

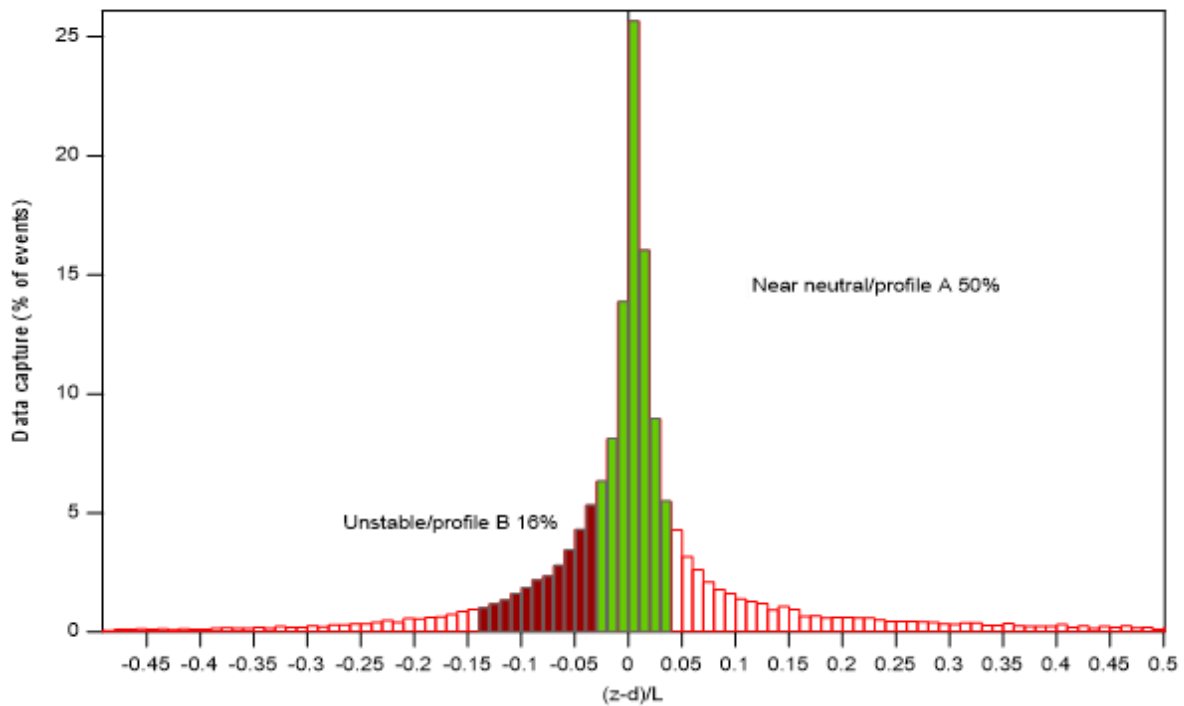


Figure 17: Distribution of the stability parameter for the period November 2021-December 2024 at Kalmthout. The coloured shades show the two COTAG profiles capture. Data presented are filtered by wind speed cut off and wind sector.

4.3 NH₃ concentrations

NH₃ mean concentrations at the two COTAG measurement heights for the near-neutral, stable and “off” profiles are shown in Figure 18 and Figure 19 for Maasmechelen and Kalmthout, respectively.

The mean concentrations represent the average of the replicate samples for A and B profiles, mostly triplicate except when outliers were removed, and the single denuder for the “off” position. Error bars represent the standard deviation for the replicate A and B samples and the uncertainty of the analytical method in the case of the “off” concentration. Due to problems with a mass flow controller in the first six measurement periods the top mean concentration for A and B was obtained with only two points at both sites. The high concentrations for B profiles at both sites for the first two measurement periods could be influenced by some source near the sampler accentuated by the very short sampling time of the B profile in those months or by contamination of the samples (handling in the lab or on the field). The large error bars show the high coefficient of variation (CV) between the replicate concentrations (in this case duplicates) for these periods. Despite a CV higher than 15% some of the concentrations for the B profile duplicates at Maasmechelen were included in the calculation as an objective criterion to decide on the outlier was not found (Figure 18, Figure 19).

Monthly concentrations of NH₃ by the COTAG were calculated as the weighted (for respective sampling duration) average of the concentrations measured at the same height (including the A, B and the “off” denuder). COTAG concentrations are shown together with NH₃ concentration measured by triplicate passive samplers at the height of the top box sampling inlet (Radiello[®], Istituti Clinici Scientifici Maugeri (<https://radiello.com/>), Sigma-Aldrich, cartridge RAD168 with diffusive body RAD1201 in adapted outdoor shelter RAD196) at the same time at the two sites in Figure 20 and Figure 21.

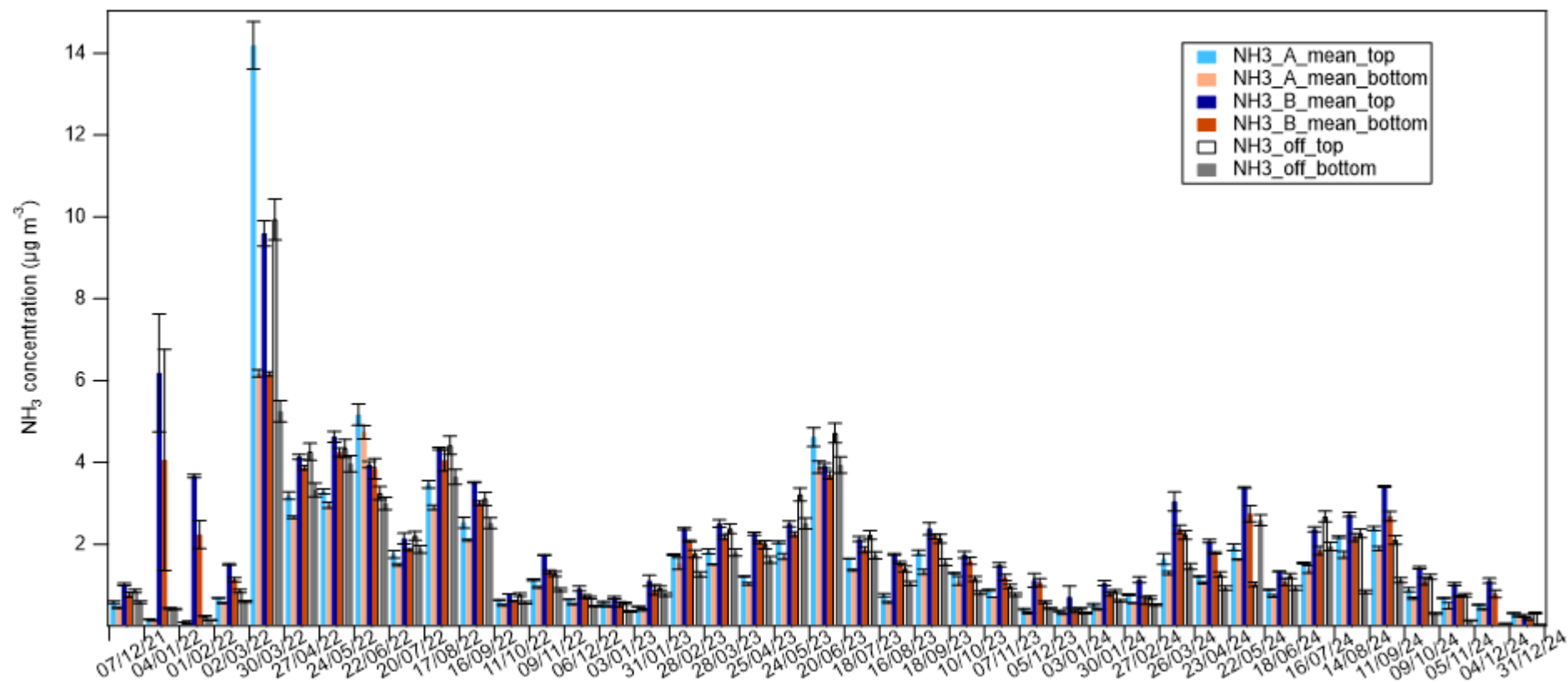


Figure 18: NH₃ mean concentration at the two sampling heights (top and bottom) for each stability class (A – near neutral, B - unstable and 'off') in Maasmechelen. Error bars represent the standard deviation of the replicate samples for A and B. In the case of the "off" concentration the error bars represent the uncertainty of the analytical method. The date on the x-axis is the end of the 4 weeks measurement period.

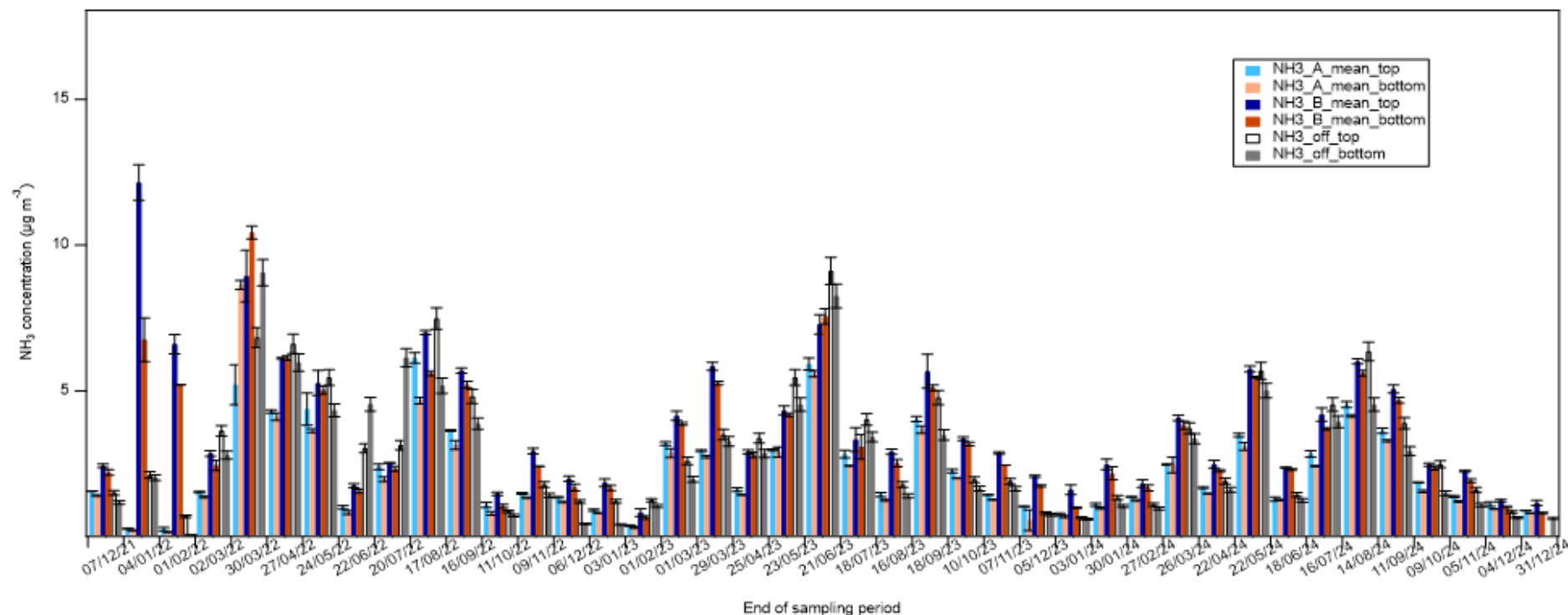


Figure 19: NH₃ mean concentration at the two sampling heights (top and bottom) for each stability class (A – near neutral, B - unstable and ‘off’) in Kalmthout. Error bars represent the standard deviation of the replicate samples for A and B (the replicates were three in most cases except when outliers were removed) and the uncertainty of the analytical method in the case of the “off” concentration. The date on the x-axis is the end of the 4 weeks measurement period.

At Maasmechelen the concentrations of the top box were in good agreement with the Radiello® with the exception of the measurement period ending on 30/03/2022, when NH₃ concentration peaked at 10.2 µg m⁻³ for the COTAG and at 6.7 µg m⁻³ for the Radiello®. Difference in concentration for this point might be related to the passive sampler being less sensitive to a potential short episode at high concentration.

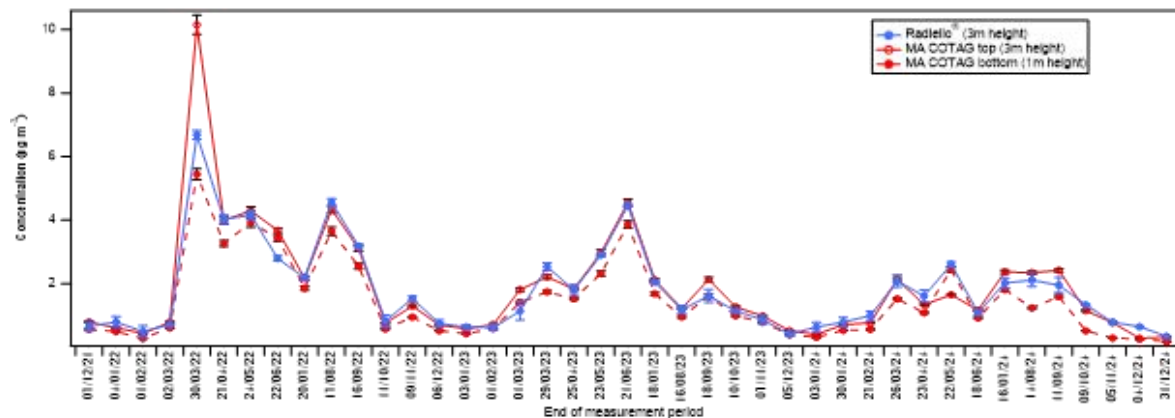


Figure 20: COTAG NH₃ concentration (COTAG = profile A + B + “off”) at both heights compared with Radiello® passive samplers at Maasmechelen (4 week average). The error bars on the COTAG measurements represent the uncertainty calculated via error propagation and on the Radiello® measurements they show the standard deviation of the triplicates.

At Kalmthout the two methods were in agreement during the winter months, but the concentration reported by the Radiello® was higher than the COTAG on three occasions during the spring and summer months of 2022 (sampling periods ending: 30/03, 27/04, 22/06/22). Since during these sampling periods the COTAG was off due to power cuts for up to 30% of the time (Figure 21), it is possible that the COTAG missed some high concentration episodes. The largest difference between the top COTAG concentration and the Radiello® measurement occurred on the period ending on 30/03/22 but no satisfactory explanation was found as a cause of the discrepancy.

Ammonia concentrations were generally slightly higher in Kalmthout compared to Maasmechelen, as expected based on the previously modelled concentrations (Figure 3), with an overall average of 2.8 µg m⁻³ and 1.7 µg m⁻³ respectively (including COTAG top and bottom concentrations for Nov 21 – Dec 24). Seasonality in concentrations was observed with values below 2 µg m⁻³ between October and March, and then increasing up to 8-10 µg m⁻³ in March. In the spring/summer period concentrations varied between 2 and 4 µg m⁻³ (Maasmechelen) and 2 and 8 µg m⁻³ (Kalmthout).

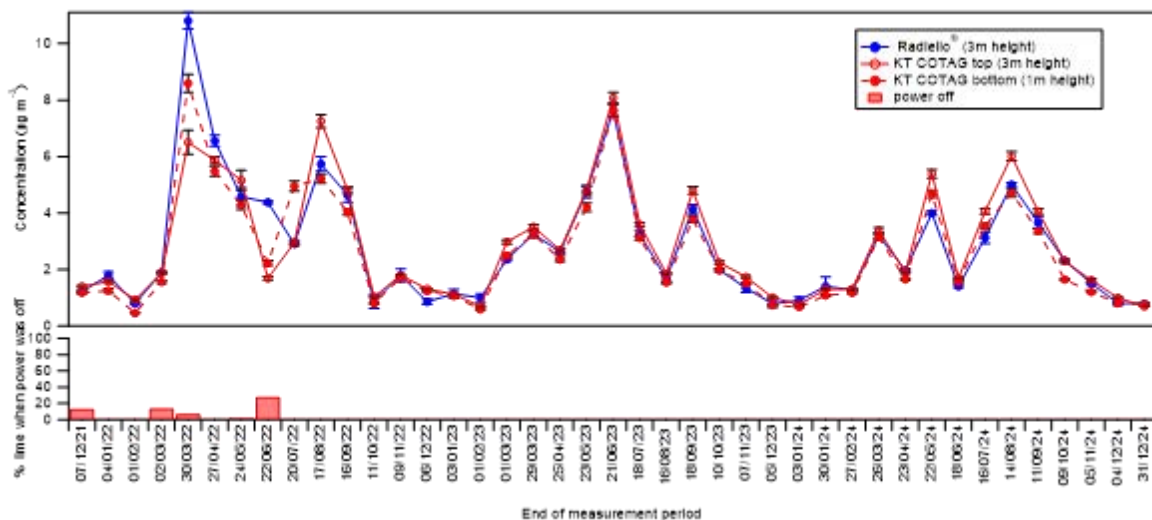


Figure 21: COTAG NH_3 concentration (COTAG = profile A + B + “off”) at both heights compared with the Radiello® passive samplers at Kalmthout (4 week average). The error bars on the COTAG measurements represent the uncertainty calculated via error propagation and on the Radiello® measurements they show the standard deviation of the triplicates.

The measured concentration gradients suggest that on average deposition took place in Maasmechelen every month (Figure 22). Positive gradients indicating deposition were observed in Kalmthout for the majority of the period with the exception of a strong negative gradient in March 2022 suggesting a potential emission event at the site (Figure 23). However, the large deposition and emission observed by the COTAG at the sites in March 2022 need to be considered cautiously and were discussed in a previous report. This is due to the unexplained discrepancy between the Radiello® and the COTAG measurements in March 2022 at each site (the latter based on only 2 denuders measurements and not 3 for this period). At both sites from October 2022 until January 2023 gradients were smaller than in summer months.

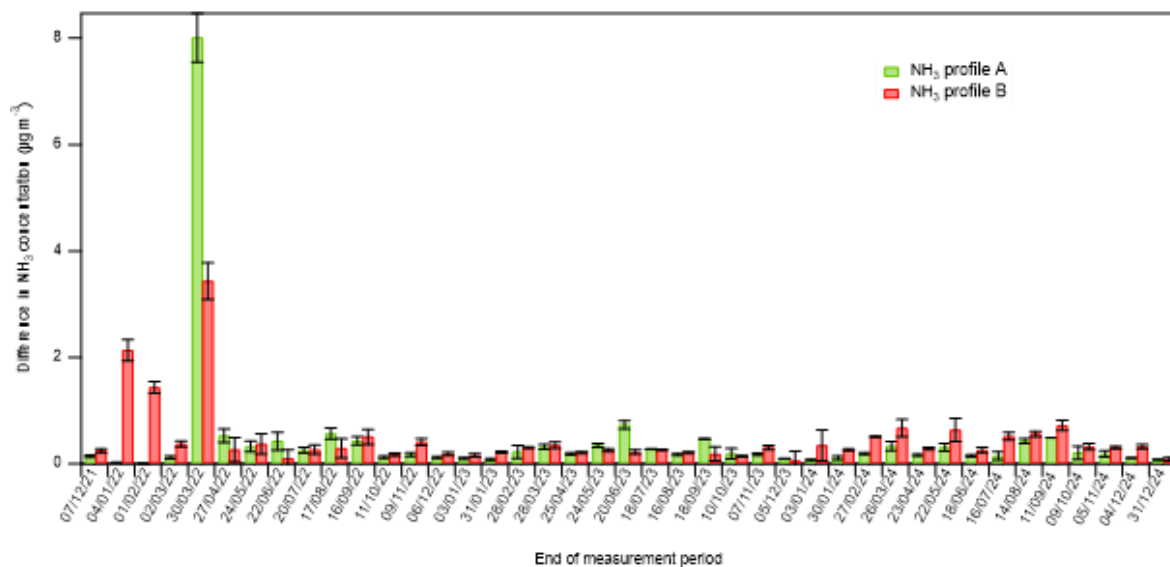


Figure 22: Difference in NH_3 concentrations between the $[\text{NH}_3]_{\text{top}}$ and $[\text{NH}_3]_{\text{bottom}}$ at Maasmechelen (4-weekly), measured by the COTAG from November 2021 to December 2024. Error bars represent the uncertainty calculated via error propagation. Profile A – near neutral, Profile B – unstable profile.

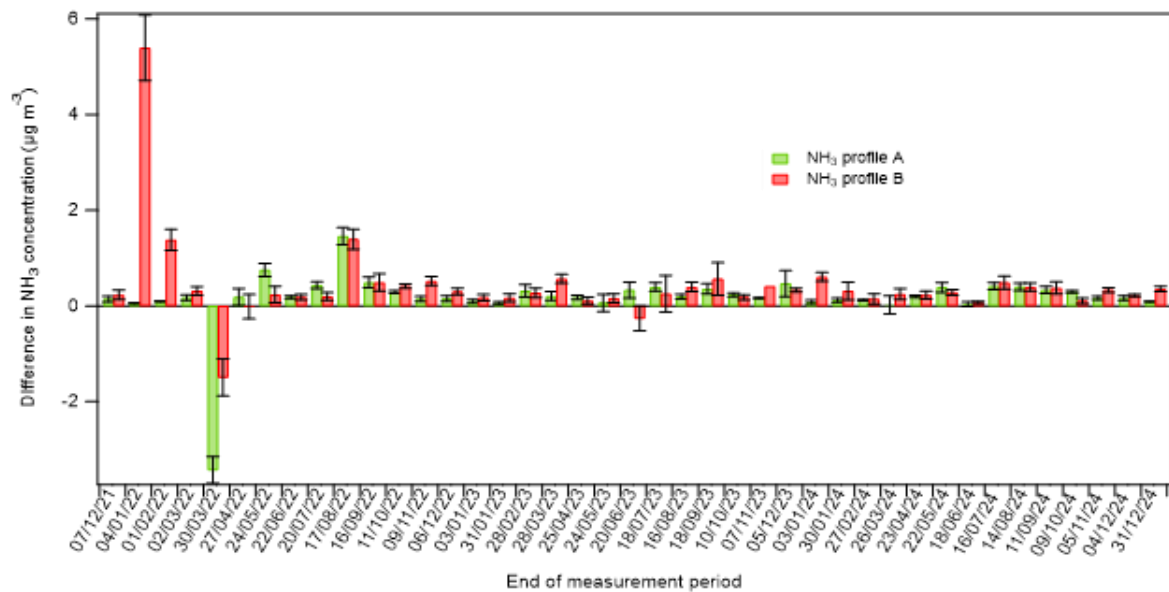


Figure 23: Difference in NH₃ concentrations between the [NH₃]_{top} and [NH₃]_{bottom} at Kalmthout (4-weekly), measured by the COTAG from November 2021 to December 2024. Error bars represent the uncertainty calculated via error propagation. Profile A – near neutral, Profile B – unstable profile.

4.4 NH₃ fluxes

Monthly flux calculations for both profiles are shown in Figure 24 and Figure 25 with the estimated errors. The measurement profiles show NH₃ deposition (negative flux) occurring from November 2021 until December 2024 in Maasmechelen (Figure 24) and in Kalmthout too, except for a single emission (positive) flux during the period ending on 30/03/22 (Figure 25). Total monthly measured net fluxes (black line in the graph) were calculated as the sum of the two profile fluxes weighted by the period they were operational as below:

$$F_{tot\ net} = 1/t \cdot (F_{COTAG\ uns\ B} \cdot t_{uns\ B} + F_{COTAG\ neu_A} \cdot t_{neu\ A}) \quad (6)$$

Where t is the total time of the measurement period (~4 weeks) and $t_{uns\ B}$ and $t_{neu\ A}$ are the times the COTAG measured under profile B and A respectively. As the flux measurement excludes highly stable conditions and periods of low wind speed, this total net flux cannot be expected to be representative of the whole period (see Section 2.1).

The overall average at Maasmechelen was $-12.3\ ng\ NH_3\ m^{-2}\ s^{-1}$ with the smallest deposition fluxes occurring between October and February with less than $-8\ ng\ m^{-2}\ s^{-1}$. Larger deposition fluxes occurred between March and September with the largest deposition in March ($-103\ ng\ m^{-2}\ s^{-1}$), most likely related to fertilisation events in the region.

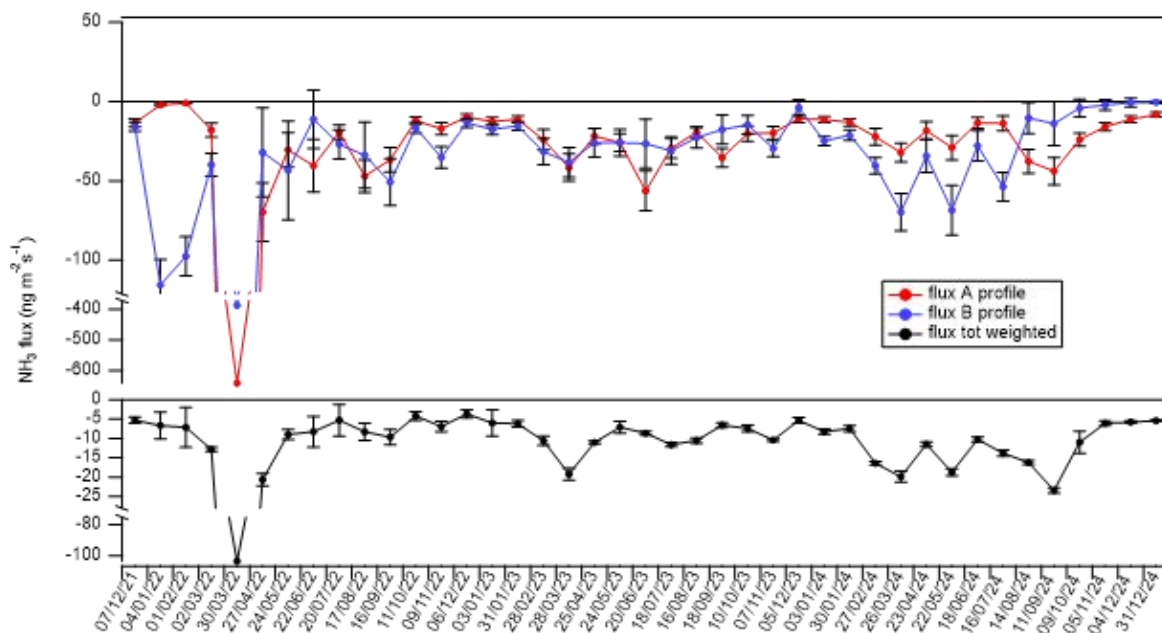


Figure 24: NH_3 fluxes at Maasmechelen. Fluxes derived from the near neutral profile are in red (A) and fluxes derived from the unstable profile are in blue (B). The total flux in black is the sum of the weighted measured fluxes (not representative of the whole period). Error bars represent the error estimated through error propagation.

At Kalmthout the overall average of the measured flux was $-10.5 \text{ ng m}^{-2} \text{ s}^{-1}$, with monthly deposition fluxes greater than $-12 \text{ ng m}^{-2} \text{ s}^{-1}$ except for the spring-summer periods, between March and August, when the deposition reduced in magnitude. One emission flux of $49 \text{ ng m}^{-2} \text{ s}^{-1}$ was measured in March 2022 and a small positive flux ($5.6 \text{ ng m}^{-2} \text{ s}^{-1}$) was recorded in June 2023. This could indicate the occurrence of bi-directional fluxes throughout the summer and that the site could be a net source of NH_3 at times.

Horizontal transport (advection) of ammonia from nearby fertilised fields or sources could introduce a bias in the measured gradient that could result in the measurement of apparent emissions or depositions from or to the studied field. The events observed in March 2022 at both sites could be influenced by advection (see section 4.4 in Di Marco et al. (2024) for a further investigation based on the calculation of the theoretical maximum dry deposition velocity).

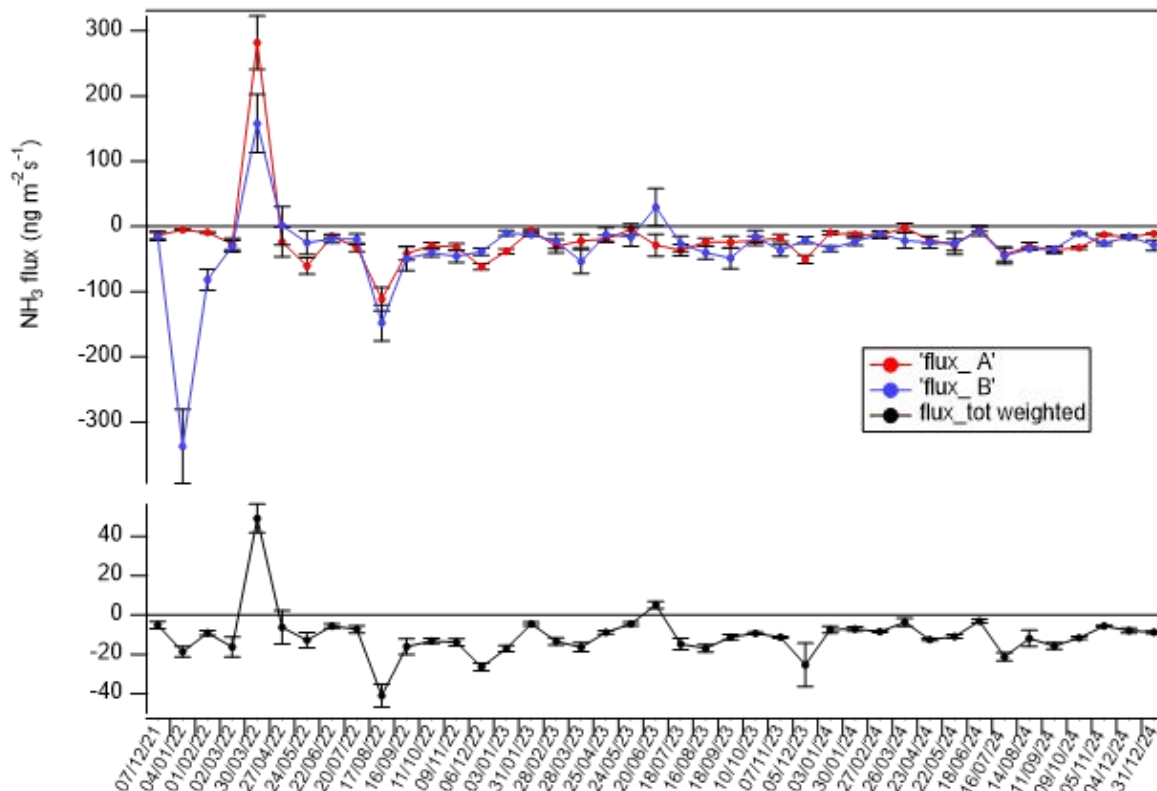


Figure 25: NH_3 fluxes at Kalmthout. Fluxes derived from the near neutral profile are in red (A) and fluxes derived from the unstable profile are in blue (B). The total flux in black is the sum of the weighted measured fluxes (not representative of the whole period). Error bars represent the error estimated through error propagation.

4.5 Gap-filled NH_3 deposition

The flux measurement does not represent a continuous measurement (with data capture at the sites ranging from 50-70% for winter months to lower values for summer months) and systematically excludes highly stable conditions and periods of low wind speed, and therefore times during which fluxes are expected to be suppressed. Thus, the magnitude of the measured net flux reported cannot be expected to be representative of the whole period. To provide an estimate of the net monthly flux, a gap-fill method designed by RIVM (Rutledge-Jonker et al., 2023) based on an extensive analysis of their historical COTAG dataset and comparison with a modelled flux was applied here. This approach was chosen as it would also make the results from the RIVM and VMM COTAGs comparable. The dry deposition was determined by multiplying the ammonia flux in a specific stability class by the time the COTAG measured under those conditions over a measurement period. The total dry deposition was defined as the sum of each term:

$$\begin{aligned}
 Dep_{tot} = & F_{\text{COTAG uns B corr}} \cdot t_{\text{uns B}} + F_{\text{COTAG neu_A corr}} \cdot t_{\text{neu A}} + \\
 & F_{\text{off uns corr}} \cdot t_{\text{off uns}} + F_{\text{off sta corr}} \cdot t_{\text{off sta}} + F_{\text{off wind}} \cdot t_{\text{off wind}} + \\
 & F_{\text{out wind sector}} \cdot t_{\text{out wind sector}}
 \end{aligned} \tag{7}$$

Where the term *corr* indicates that the flux was corrected for the cross-term following the methodology described in Section 2.6. In this method the fluxes for the period of

time when the COTAG did not measure were estimated using the fluxes from the neighbouring stability classes applying some coefficients in the following way:

off too unstable	$F_{\text{off uns corr}} \approx a_1 F_{\text{COTAG uns B corr}}$ with $a_1 \approx 1.1$
off too stable	$F_{\text{off sta corr}} \approx a_2 F_{\text{COTAG neu A corr}}$ with $a_2 \approx 0.4$
off too little wind	$F_{\text{off wind}} \approx 0$
off out of wind sector	$F_{\text{out wind sector}} = \langle F_{\text{COTAG uns B corr}} \cdot t_{\text{uns B}} + F_{\text{COTAG neu A corr}} \cdot t_{\text{neu A}} + F_{\text{off uns corr}} \cdot t_{\text{off uns}} + F_{\text{off sta corr}} \cdot t_{\text{off sta}} \rangle \cdot 1 / (t_{\text{uns B}} + t_{\text{neu A}} + t_{\text{off uns}} + t_{\text{off sta}})$

Here the parameters a_1 and a_2 were taken from the analysis of Rutledge-Jonker et al. (2023) who numerically simulated the COTAG protocol using an hourly modelled time-series of the exchange. Applying the described approach to the Belgian sites a gap-filled flux was obtained and the deposition was plotted in Figure 26 and Figure 27 as a combination of all the components listed above.

The average 4-weekly deposition at Maasmechelen was $-0.47 \pm 0.08 \text{ kg NH}_3 \text{ ha}^{-1}$ and $-0.35 \pm 0.08 \text{ kg NH}_3 \text{ ha}^{-1}$ if the single period with possible advection in March 2022 was excluded and an average value of interpolation (average of the previous and following periods) was used instead (Figure 28).

At Kalmthout the mean 4-weekly flux was $-0.29 \pm 0.12 \text{ kg NH}_3 \text{ ha}^{-1}$ and $-0.35 \pm 0.11 \text{ kg NH}_3 \text{ ha}^{-1}$ if the period in March 2022 with net emission was excluded (Figure 28). Table 6 shows the gap-filled 4-weekly depositions.

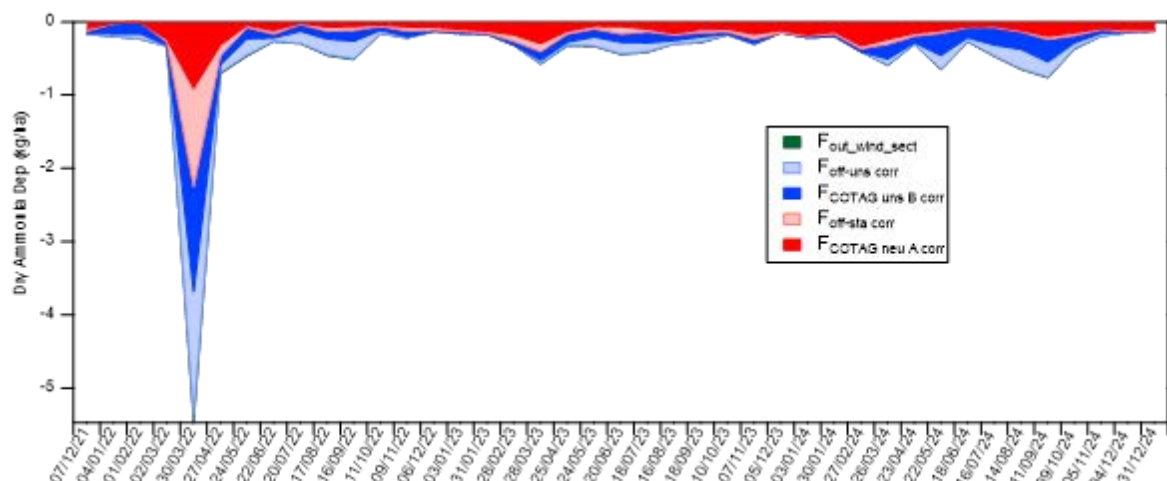


Figure 26: Gap-filled ammonia (component) fluxes at Maasmechelen.

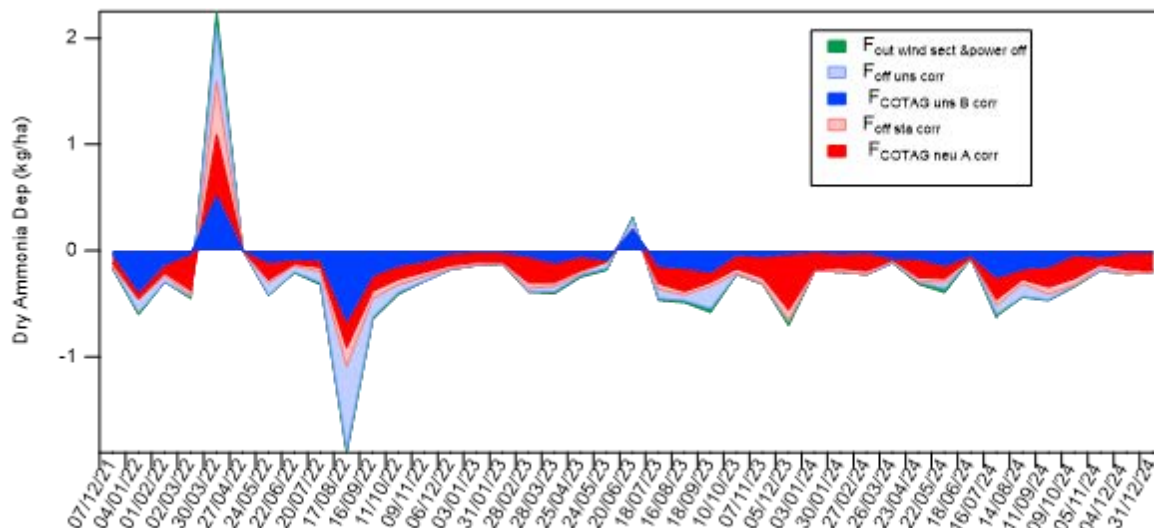


Figure 27: Gap-filled ammonia (component) fluxes at Kalmthout.

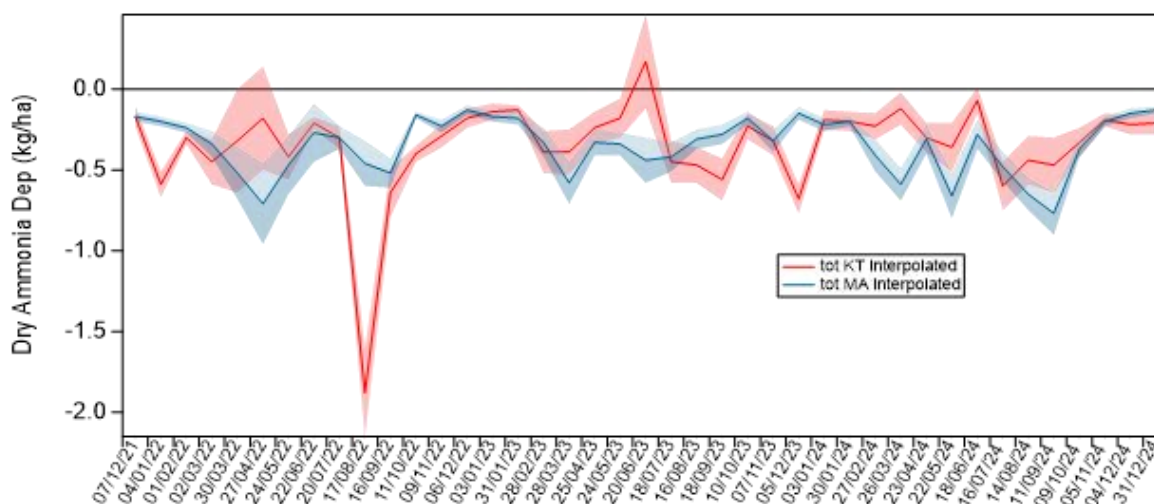


Figure 28: Total ammonia deposition at Maasmechelen and Kalmthout using interpolation data for March 2022.

The sampling period considered in this report is 09/11/2021 to 31/12/2024, so a total of 1147 days (3.1 years). The total summed gap-filled deposition in this period was 19.14 kg NH₃ ha⁻¹ at Maasmechelen and 11.77 kg NH₃ ha⁻¹ at Kalmthout. Using the interpolated values (reported as a note in Table 6) for the period in March 2022 (01/03 to 29/03/2022) the total deposition in 3.1 years was 14.20 kg NH₃ ha⁻¹ at Maasmechelen and 14.27 kg NH₃ ha⁻¹ at Kalmthout.

At Maasmechelen the net dry deposition for the first three fully measured calendar years using the interpolated value for March 2022 and accounting for the included number of sampling days, was 4.5, 4.1 and 5.2 kg NH₃ ha⁻¹ year⁻¹ for 2022, 2023 and 2024 respectively. At Kalmthout the dry deposition for 2022, 2023 and 2024 was 5.8, 4.0 and 3.8 kg NH₃ ha⁻¹ year⁻¹ respectively. Expressed as kilogram nitrogen in ammonia gas, this corresponds in 2022, 2023 and 2024 to 3.7, 3.4 and 4.3 kg NH₃-N ha⁻¹ year⁻¹ at Maasmechelen and 4.8, 3.3 and 3.1 kg NH₃-N ha⁻¹ year⁻¹ at Kalmthout.

4.6 Wind profile study

4.6.1 Methodology

The uncertainty on the displacement value d contributes to the uncertainty on the flux (cf. Section 2.6). Therefore, wind profile measurements at five heights were carried out at the 2 COTAG sites. Cup anemometers (A100R from Vector Instruments) were mounted on 5 horizontal arms attached to a metal pole (2.7 m height, 3 cm diameter) (Figure 29) to provide wind speed measurements. The measurements were logged and 30-minute averages were saved on a separate Campbell datalogger (LoggerNet software) in a weatherproof box at the foot of the pole. Power (12 V) was obtained from the main power box. The setup was installed a few meters west of the COTAG mast.



Figure 29: Pole with 5 cup anemometers and datalogger box at Kalmthout.

These wind measurements were used to calculate d based on the expected linear relationship between the horizontal wind speed at height z (u_z) and the logarithm of $(z - d)$ under neutral stability conditions ($L > 100$ m and $L < -200$ m) and high winds ($u^* > 0.5$ m/s or $u^* > 1$ m/s). (Figure 30). With these conditions, the displacement height was obtained after an iterative process to optimise the linear relationship for each 30-min wind speed profile using both Excel and a script in R.

$$u_z = \frac{u_*}{\kappa} \left[\ln \left(\frac{z - d}{z_0} \right) \right] \quad (8)$$

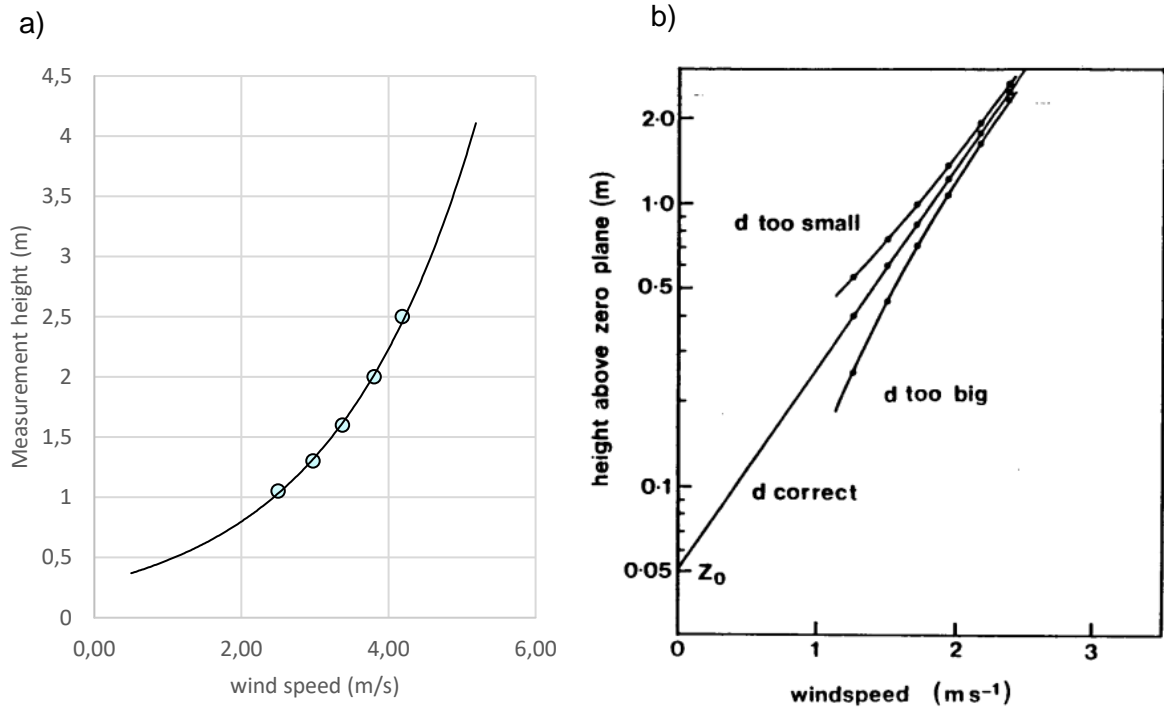


Figure 30: Example of half-hour wind profile measured at Maasmechelen (a) and effect of the estimate of zero plane displacement on the logarithmic wind profile in neutral conditions (Stull, 1988) (b).

4.6.2 Maasmechelen

In the case of Maasmechelen the vegetation height was difficult to determine for the slight heterogeneity of the vegetation and soil. The overall heathland height southwest of the COTAG mast was visually estimated to be 0.90 cm above soil level, without a clear difference between seasons (July vs. Nov 2023) and years (summer 2023 vs. 2024). A wind profile study measuring wind speeds at 5 heights (1.05, 1.3, 1.6, 2.0 and 2.5 m above soil level) using cup anemometers was carried out at the site between 13 September 2023 and 26 March 2024.

Half-hourly values of the calculated d are shown in Figure 31. Although quite a lot of variation can be observed in the time series, a clear seasonal variation was not observed.

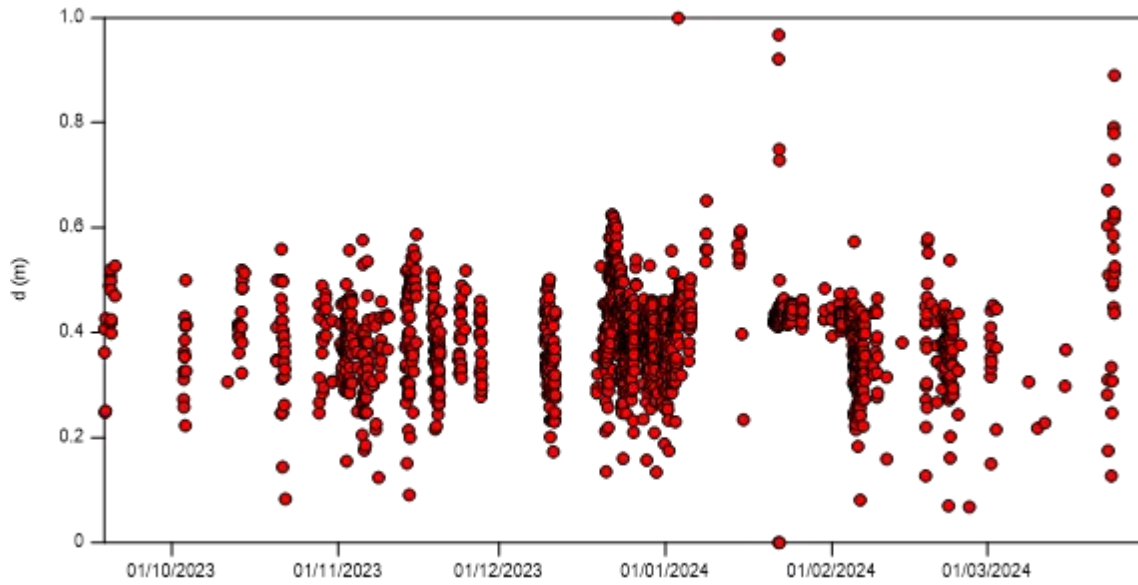


Figure 31: Time series of the displacement height d calculated every 30 min at Maasmechelen over the period September 2023 - March 2024. Data analysed for neutral conditions only with $L > 100$ m and $L < -200$ m and $u^* > 0.5$ m/s.

A distribution of d is shown in Figure 32. The average value for the measurement period was 0.39 ± 0.09 m, whereas the default value obtained from the canopy height ($0.65 \times h_{\text{canopy}}$) and used in the COTAG flux calculation was 0.585 m. The new value of d suggests that at this field site, the displacement height represents 44% of the canopy height and not 65% as assumed, at least based on the visually estimated h_{canopy} of 0.90 m.

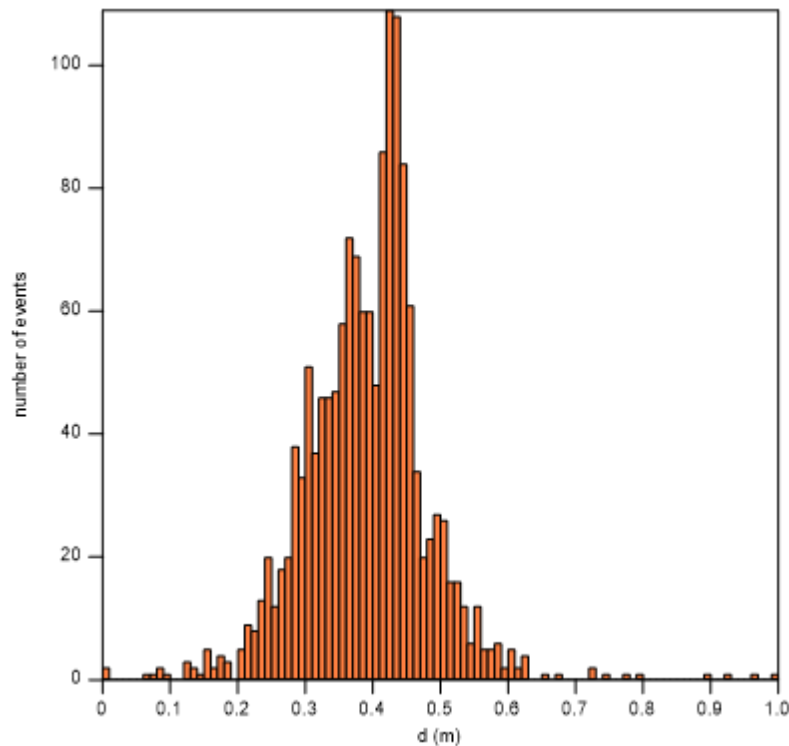


Figure 32: Distribution of d over the wind profile measurements at Maasmechelen.

Although d can vary depending on the wind direction, in Maasmechelen the wind direction was mostly from the sector 150° - 330° , and the other wind sectors did not have much influence on d (Figure 33).

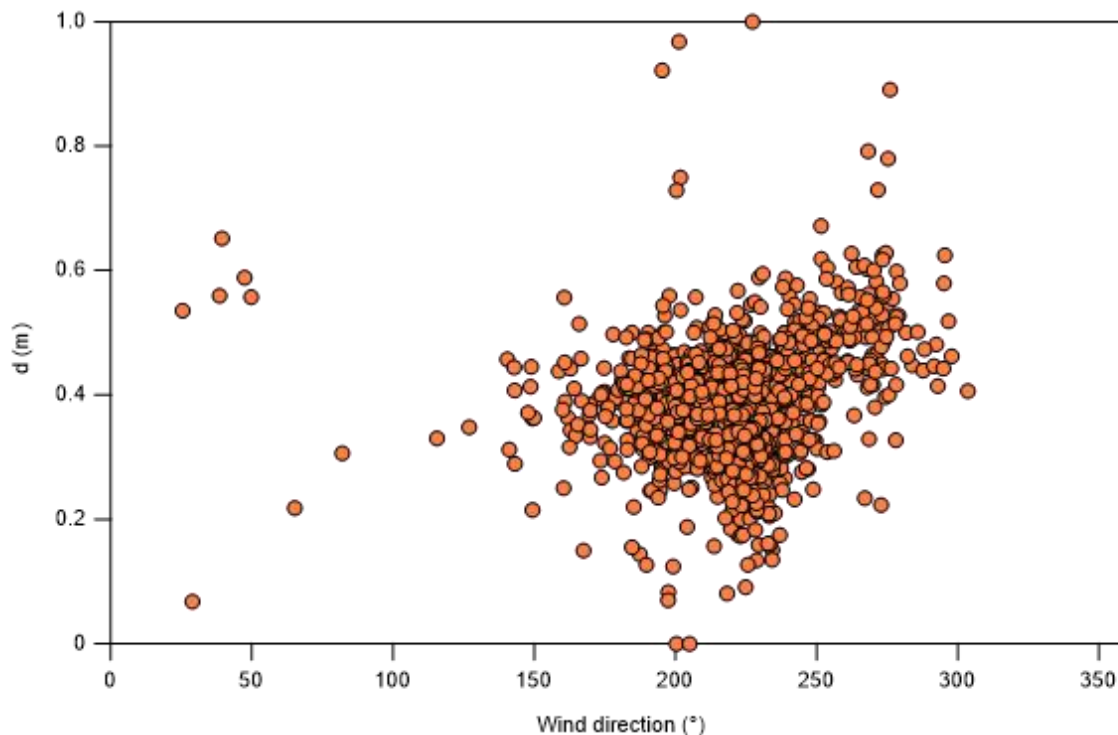


Figure 33: Variation of d depending on the wind direction (wind sectors excluded for the COTAG measurements were also excluded in this analysis).

4.6.3 Kalmthout

In Kalmthout the vegetation height was 0.80 cm above soil level without a clear difference between seasons. Unlike Maasmechelen, the canopy height was more straightforward to measure and assess. A wind profile study measuring wind speeds at 5 heights (1.09, 1.36, 1.63, 2.05 and 2.52 m above soil level) using cup anemometers was carried out at the site between 22 April 2024 and 29 January 2025. The calculated d showed a lot of variation, but a clear seasonal variation was not observed (Figure 34).

The displacement height did not show any dependency on wind direction (Figure 35).

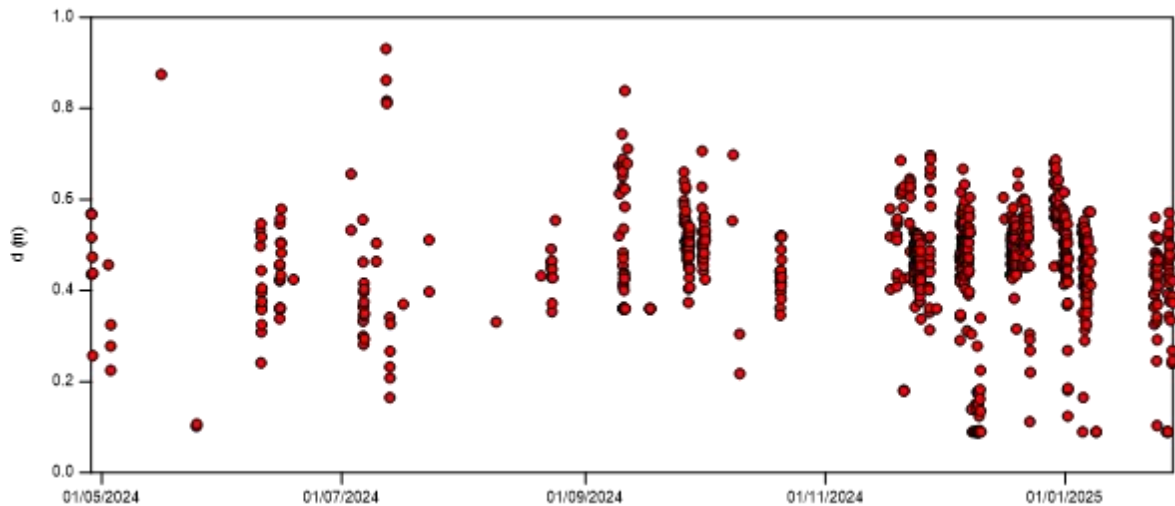


Figure 34: Time series of the displacement height d calculated every 30 min at Kalmthout over the period April 2024 - January 2025. Data shown were filtered for neutral conditions only with $L > 100$ m and $L < -200$ m and $u^* > 0.5$ m/s.

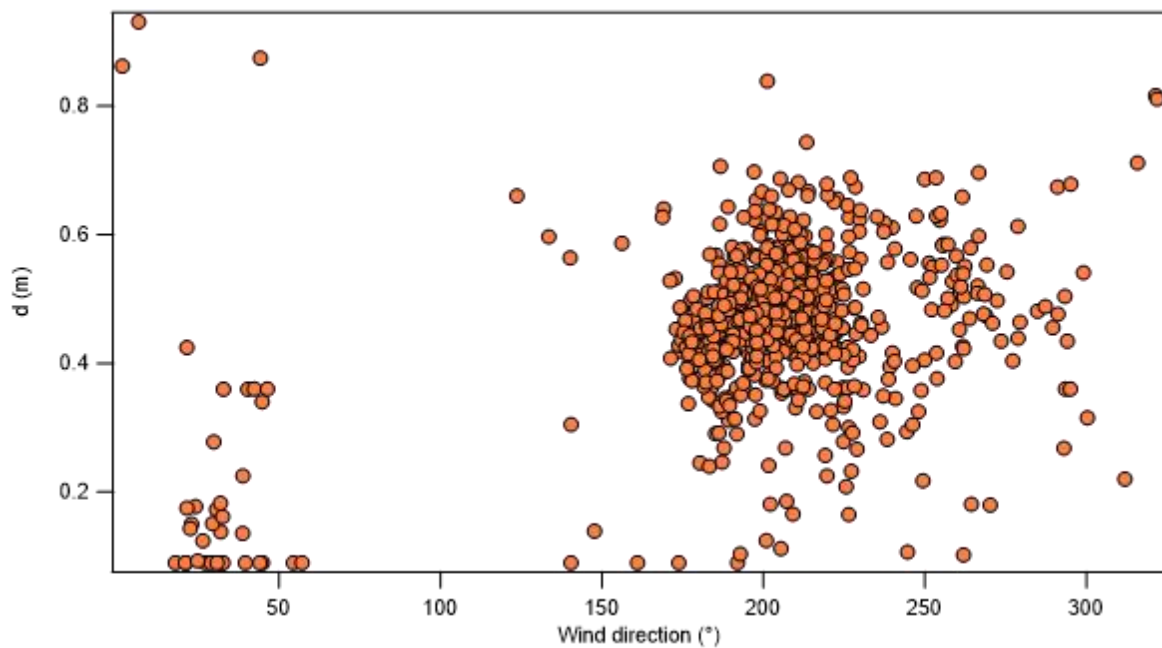


Figure 35: Variation of d depending on the wind direction (wind sectors excluded for the COTAG measurements were also excluded in this analysis).

The calculation of d was filtered for cases with $u^* > 0.5$ m/s and also with the stricter condition of $u^* > 1$ m/s to look at windier conditions with neutral stability that should provide clearer logarithmic profiles of the wind speed. The average value for the measurement period was 0.46 ± 0.12 m in the first case and 0.50 ± 0.15 m in the second case (Table 5). If considering the second value of d , this would represent 63% of the canopy height (0.80 m), slightly lower than the value (0.52 m) adopted so far at Kalmthout. The u^* filter did not make a significant difference in the calculation of d for Maasmechelen (Table 5).

Table 5 Summary of the calculation of the displacement height d (m) for Maasmechelen and Kalmthout.

d	Maasmechelen		Kalmthout	
	$u^* > 0.5$ m/s	$u^* > 1$ m/s	$u^* > 0.5$ m/s	$u^* > 1$ m/s
<i>Average</i>	0.39	0.39	0.46	0.50
<i>Median</i>	0.40	0.39	0.47	0.54
<i>St dev</i>	0.09	0.08	0.12	0.15
<i>N of points</i>	1477	96	756	78

The influence on the NH₃ deposition of the change in d was assessed by recalculating the COTAG fluxes. The newly obtained 4-weekly values for Maasmechelen show a deposition larger than previously estimated (Table 6). Overall, the change in d had an effect of about 17% of the deposition estimates. This is slightly higher but comparable to the 15% effect on the deposition as estimated by Rutledge-Jonker et al. (2023) for a bias of $(z-d)$ of 0.2 m. In the case of Kalmthout the newly obtained depositions (with a d value of 0.5 m) were 2% higher than previous estimates.

Table 6: Monthly deposition at Kalmthout and Maasmechelen. Negative values indicate deposition, positive values indicate emissions.

Measurement period		Kalmthout	New $d = 0.50$ Kalmthout	Maasmechelen	New $d = 0.39$ Maasmechelen
Start	End	(kg NH ₃ ha ⁻¹)			
09/11/2021	07/12/2021	-0.17 ± 0.06	-0.17 ± 0.06	-0.17 ± 0.03	-0.21 ± 0.03
07/12/2021	04/01/2022	-0.59 ± 0.08	-0.60 ± 0.09	-0.20 ± 0.03	-0.25 ± 0.03
04/01/2022	01/02/2022	-0.30 ± 0.04	-0.30 ± 0.04	-0.24 ± 0.03	-0.29 ± 0.04
01/02/2022	01/03/2022	-0.45 ± 0.14	-0.46 ± 0.15	-0.34 ± 0.08	-0.40 ± 0.10
01/03/2022	29/03/2022	2.19 ± 0.34*	2.24 ± 0.35*	-5.47 ± 0.67**	-6.60 ± 0.84***
29/03/2022	26/04/2022	-0.18 ± 0.32	-0.19 ± 0.32	-0.71 ± 0.25	-0.86 ± 0.33
26/04/2022	24/05/2022	-0.42 ± 0.15	-0.43 ± 0.15	-0.47 ± 0.18	-0.58 ± 0.41
24/05/2022	21/06/2022	-0.21 ± 0.05	-0.22 ± 0.05	-0.27 ± 0.18	-0.33 ± 0.34
21/06/2022	19/07/2022	-0.30 ± 0.08	-0.31 ± 0.08	-0.30 ± 0.07	-0.37 ± 0.08
19/07/2022	16/08/2022	-1.88 ± 0.29	-1.93 ± 0.30	-0.46 ± 0.14	-0.57 ± 0.17
16/08/2022	13/09/2022	-0.64 ± 0.15	-0.65 ± 0.16	-0.52 ± 0.09	-0.61 ± 0.11
13/09/2022	12/10/2022	-0.40 ± 0.05	-0.41 ± 0.05	-0.16 ± 0.02	-0.20 ± 0.03
12/10/2022	07/11/2022	-0.29 ± 0.07	-0.29 ± 0.07	-0.23 ± 0.04	-0.27 ± 0.05
07/11/2022	07/12/2022	-0.18 ± 0.06	-0.19 ± 0.06	-0.13 ± 0.03	-0.16 ± 0.03
07/12/2022	03/01/2023	-0.14 ± 0.05	-0.14 ± 0.05	-0.17 ± 0.03	-0.20 ± 0.04
03/01/2023	31/01/2023	-0.13 ± 0.03	-0.13 ± 0.03	-0.18 ± 0.04	-0.21 ± 0.04
31/01/2023	28/02/2023	-0.39 ± 0.13	-0.40 ± 0.13	-0.33 ± 0.09	-0.39 ± 0.11
28/02/2023	28/03/2023	-0.39 ± 0.15	-0.40 ± 0.15	-0.58 ± 0.13	-0.70 ± 0.15
28/03/2023	25/04/2023	-0.24 ± 0.10	-0.24 ± 0.10	-0.33 ± 0.08	-0.40 ± 0.10
25/04/2023	24/05/2023	-0.18 ± 0.12	-0.18 ± 0.13	-0.34 ± 0.07	-0.41 ± 0.09
24/05/2023	20/06/2023	0.17 ± 0.30	0.18 ± 0.31	-0.44 ± 0.14	-0.54 ± 0.17
20/06/2023	18/07/2023	-0.45 ± 0.13	-0.46 ± 0.13	-0.42 ± 0.09	-0.51 ± 0.11
18/07/2023	16/08/2023	-0.47 ± 0.12	-0.48 ± 0.12	-0.31 ± 0.06	-0.37 ± 0.08
16/08/2023	18/09/2023	-0.56 ± 0.14	-0.57 ± 0.14	-0.28 ± 0.06	-0.34 ± 0.08
18/09/2023	10/10/2023	-0.23 ± 0.08	-0.23 ± 0.08	-0.18 ± 0.04	-0.22 ± 0.05
10/10/2023	07/11/2023	-0.32 ± 0.09	-0.32 ± 0.09	-0.32 ± 0.07	-0.38 ± 0.08
07/11/2023	05/12/2023	-0.68 ± 0.09	-0.70 ± 0.09	-0.15 ± 0.04	-0.18 ± 0.04
05/12/2023	03/01/2024	-0.19 ± 0.06	-0.20 ± 0.06	-0.22 ± 0.04	-0.26 ± 0.05
03/01/2024	30/01/2024	-0.20 ± 0.06	-0.21 ± 0.06	-0.20 ± 0.03	-0.24 ± 0.04
30/01/2024	27/02/2024	-0.23 ± 0.08	-0.23 ± 0.08	-0.41 ± 0.10	-0.49 ± 0.12
27/02/2024	26/03/2024	-0.12 ± 0.10	-0.12 ± 0.10	-0.59 ± 0.10	-0.71 ± 0.12
26/03/2024	23/04/2024	-0.30 ± 0.09	-0.30 ± 0.09	-0.31 ± 0.09	-0.38 ± 0.11
23/04/2024	21/05/2024	-0.36 ± 0.15	-0.36 ± 0.15	-0.66 ± 0.14	-0.81 ± 0.17
21/05/2024	18/06/2024	-0.07 ± 0.08	-0.08 ± 0.08	-0.28 ± 0.09	-0.35 ± 0.11
18/06/2024	16/07/2024	-0.60 ± 0.15	-0.61 ± 0.16	-0.48 ± 0.09	-0.58 ± 0.11
17/07/2024	14/08/2024	-0.44 ± 0.15	-0.45 ± 0.15	-0.65 ± 0.10	-0.80 ± 0.13
14/08/2024	11/09/2024	-0.47 ± 0.17	-0.48 ± 0.17	-0.77 ± 0.13	-0.94 ± 0.16
11/09/2024	09/10/2024	-0.33 ± 0.09	-0.34 ± 0.09	-0.37 ± 0.05	-0.44 ± 0.07
09/10/2024	06/11/2024	-0.19 ± 0.04	-0.20 ± 0.04	-0.20 ± 0.03	-0.24 ± 0.03
06/11/2024	04/12/2024	-0.22 ± 0.06	-0.23 ± 0.06	-0.15 ± 0.03	-0.18 ± 0.03
04/12/2024	30/12/2024	-0.21 ± 0.07	-0.22 ± 0.07	-0.13 ± 0.02	-0.16 ± 0.03

* Value excluded in calculation; replaced by interpolation value of -0.32 ± 0.23

** Value excluded in calculation; replaced by interpolation value of -0.52 ± 0.16

*** Value excluded in calculation; replaced by interpolation value of -0.63 ± 0.21

5 Conclusions & recommendations

The COTAG NH₃ concentrations showed good agreement with the concentrations reported by the passive samplers. This suggests that the COTAG systems worked well and gives confidence in the COTAG concentration profiles for the periods studied. The initial problems in regulating the airflows appear to be resolved and for most months the triplicate denuders have been used to estimate the average concentrations, as the CV was below 15 %. The change in stability window implemented in July 2023 has provided an average increase in data capture to 50-60% at both sites, making the COTAG results more robust.

For the measurement period presented (Nov 2021 – December 2024; 1147 days or 3.1 years), Maasmechelen consistently reported a net deposition flux for each 4-weekly sampling period resulting in a total deposition of 14.20 kg NH₃ ha⁻¹. The new value of displacement height suggested that the deposition at Maasmechelen could be up to 17% higher at 17.12 kg NH₃ ha⁻¹ for the 3.1 year period. Kalmthout observed some emissions together with deposition events and slightly higher NH₃ concentrations compared to Maasmechelen. This is likely to indicate that fluxes of NH₃ at this site could be bi-directional during the warm months. The total deposition at Kalmthout in Nov 2021 – December 2024 was 14.27 kg NH₃ ha⁻¹. The implementation of the new *d* made only a 2% increase in the calculation of the deposition with a total of 14.59 kg NH₃ ha⁻¹. This could be attributed to the fact that in Kalmthout the canopy height measurement is more certain and easier to carry out than in Maasmechelen. This work confirms the importance of canopy measurement for the calculation of fluxes via gradient.

In the first three fully measured calendar years 2022-2023-2024, the net dry deposition was 4.5, 4.1 and 5.2 kg NH₃ ha⁻¹ year⁻¹ at Maasmechelen and 5.8, 4.0 and 3.8 kg NH₃ ha⁻¹ year⁻¹ at Kalmthout. Expressed as kilogram nitrogen in ammonia, this corresponds to 3.7, 3.4 and 4.3 kg NH₃-N ha⁻¹ year⁻¹ at Maasmechelen, and 4.8, 3.3 and 3.1 kg NH₃-N ha⁻¹ year⁻¹ at Kalmthout.

The wind profile study at Maasmechelen showed that a bias on displacement height *d* of ~0.2 m could introduce an uncertainty of about 17% on the total flux calculation, suggesting that *d* could be the main source of uncertainty in a gradient flux calculation. The study of *d* in Kalmthout provided a value close to the previously adopted displacement height of 0.52 m, with a consequent small (2%) increase on the flux calculation. The new *d* values should be used in the logging programs of the COTAG at the two sites.

It must be noted that the methodology for gap-filling and cross-term correction is based on model simulations of fluxes at the Dutch sites: there is therefore an uncertainty related to the assumption that the relationship is still valid for the Belgian sites.

For future studies, a comparison of the NH₃ deposition estimated by COTAG with modelled annual deposition by different models could be useful in investigating the parametrization of deposition velocities to these types of land cover and ecosystems.

Bibliography

- Di Marco C., Staelens J. (2022) Dry deposition measurements of ammonia at two heathland sites in Flanders (Nov 2021-Oct 2022) - Site selection study. UK Centre for Ecology & Hydrology. Study on behalf of Flanders Environment Agency.
- Di Marco C., Staelens J., Twigg M., Stephens A., Nemitz E. (2024) Dry deposition measurements of ammonia at two heathland sites in Flanders (Nov 2021 – July 2023). UK Centre for Ecology & Hydrology. Study on behalf of Flanders Environment Agency.
- Dyer A.J., Hicks B.B. (1970) Flux-gradient relationships in the constant flux layer. *Quarterly Journal of the Royal Meteorological Society* 96, 715-721. <https://doi.org/10.1002/qj.49709641012>.
- Flechard C.R. (1998) Turbulent exchange of ammonia above vegetation. PhD thesis, University of Nottingham, UK.
- Foken T. (2008) *Micrometeorology*. Springer Berlin. <https://doi.org/10.1007/978-3-540-74666-9>.
- Garratt J. (1994) Review: the atmospheric boundary layer. *Earth-Science Reviews* 37, 89-134. [https://doi.org/10.1016/0012-8252\(94\)90026-4](https://doi.org/10.1016/0012-8252(94)90026-4).
- Kaimal J.C., Finnigan J.J. (1994) *Atmospheric boundary layer flows. Their structure and measurements*. Oxford University Press, New York. <https://doi.org/10.1093/oso/9780195062397.001.0001>.
- Monteith J., Unsworth M.H. (2013) *Principles of environmental physics: plants, animals, and the atmosphere*. Elsevier. <https://doi.org/10.1016/C2010-0-66393-0>.
- Neiryneck J., Kowalski A.S., Carrara A., Ceulemans R. (2005) Driving forces for ammonia fluxes over mixed forest subjected to high deposition loads. *Atmospheric Environment* 39, 5013-5024. <https://doi.org/10.1016/j.atmosenv.2005.05.027>.
- Neiryneck J., Kowalski A.S., Carrara A., Genouw G., Berghmans P., Ceulemans R. (2007) Fluxes of oxidised and reduced nitrogen above a mixed coniferous forest exposed to various nitrogen emission sources. *Environmental Pollution* 149, 31-43. <https://doi.org/10.1016/j.envpol.2006.12.029>.
- Rutledge-Jonker S., Braam M., Hoogerbrugge R., Wichink Kruit R., Nemitz E. et al. (2023) Ammonia deposition measured with Conditional Time-Averaged Gradient (COTAG) systems in the Netherlands. Methodological advances and results for 2012-2020. National Institute for Public Health and the Environment (RIVM). <https://dx.doi.org/10.21945/RIVM-2022-0202>.
- Stull R.B. (ed.) (1998) *An introduction to boundary layer meteorology*. Atmospheric and Oceanographic Sciences Library, volume 13. Springer Dordrecht. <https://doi.org/10.1007/978-94-009-3027-8>.
- Tang Y.S., Braban C.F., Dragosits U., Simmons I., Leaver D. et al. (2018) Acid gases and aerosol measurements in the UK (1999–2015): regional distributions and trends. *Atmospheric Chemistry and Physics* 18, 16293-16324. <https://doi.org/10.5194/acp-18-16293-2018>.

- Tang Y.S., Dragosits U., van Dijk N., Love L., Simmons I., Sutton M.A. (2009) Assessment of ammonia and ammonium trends and relationship to critical levels in the UK National Ammonia Monitoring Network (NAMN). In: Sutton M., Reis S., Baker S.M.H. (eds.), Atmospheric Ammonia - Detecting emission changes and environmental impacts. Results of an Expert Workshop under the Convention on Long-range Transboundary Air Pollution. Springer, 187-194. <https://doi.org/10.1007/978-1-4020-9121-6>.
- Webb E.K. (1970) Profile relationships: the log-linear range, and extension to strong stability. Quarterly Journal of the Royal Meteorological Society 96, 67-90. <https://doi.org/10.1002/qj.49709640708>.



BANGOR

UK Centre for Ecology & Hydrology
Environment Centre Wales
Deiniol Road
Bangor
Gwynedd
LL57 2UW
United Kingdom
T: +44 (0)1248 374500
F: +44 (0)1248 362133

EDINBURGH

UK Centre for Ecology & Hydrology
Bush Estate
Penicuik
Midlothian
EH26 0QB
United Kingdom
T: +44 (0)131 4454343
F: +44 (0)131 4453943

LANCASTER

UK Centre for Ecology & Hydrology
Lancaster Environment Centre
Library Avenue
Bailrigg
Lancaster
LA1 4AP
United Kingdom
T: +44 (0)1524 595800
F: +44 (0)1524 61536

WALLINGFORD (Headquarters)

UK Centre for Ecology & Hydrology
Maclean Building
Benson Lane
Crowmarsh Gifford
Wallingford
Oxfordshire
OX10 8BB
United Kingdom
T: +44 (0)1491 838800
F: +44 (0)1491 692424

enquiries@ceh.ac.uk

www.ceh.ac.uk